Preprints (www.preprints.org) | NOT PEER-REVIEWED | Posted: 25 January 2018 doi:10.20944/preprints201801.0238.v1

Peer-reviewed version available at Int. J. Mol. Sci. 2018, 19, 837; doi:10.3390/ijms19030837

Article

Combined Subchronic Toxicity of Aluminum (III), Titanium (IV) and Silicon (IV) Oxide Nanoparticles and Its Alleviation with a Complex of Bioprotectors

Ilzira A. Minigalieva[1], Boris A. Katsnelson[1]*, Larisa I. Privalova[1], Marina P. Sutunkova[1], Vladimir B. Gurvich[1], Vladimir Y. Shur[2], Ekaterina V. Shishkina[2], Irene E. Valamina[3], Oleg H. Makeyev[3], Vladimir G. Panov[4], Anatoly N. Varaksin[4], Tatiana V. Bushueva[1], Renata R. Sakhautdinova[1], Svetlana V. Klinova[1], Svetlana N. Solovyeva[1], Ekaterina Y. Meshtcheryakova[3]

[1] The Medical Research Center for Prophylaxis and Health Protection in Industrial Workers, 30 Popov Str., Ekaterinburg 620014, Russia; e-mails: ilzira-minigalieva@yandex.ru (I.A.M.); privalovali@yahoo.com (L.I.P.); marinasutunkova@yandex.ru (M.P.S.); gurvich@ymrc.ru (V.B.G.); bushueva@ymrc.ru (T.V.B); sahautdinova@ymrc.ru (R.R.S); klinova@ymrc.ru (S.V.K.); solovyeva@ymrc.ru (S.N.S.)

[2] The Institute of Natural Sciences, The Ural Federal University, Ekaterinburg 620000, Russia; E-mails: vladimir.shur@urfu.ru (V.Y.S.); ekaterina.shishkina@labfer.usu.ru (E.V.S.)

[3] The Central Research Laboratory, The Ural State Medical University, 17 Klyuchevskaya Str., Ekaterinburg 620109, Russia; e-mails: ivalamina@mail.ru (I.E.V.); ommt305@mail.ru (O.H.M.); katusha-ugma@rambler.ru (E.Y.M.)

[4] Institute of Industrial Ecology, the Urals Branch of the Russian Academy of Sciences, 20 Sofia Kovalevskaya Str., Ekaterinburg 620990, Russia; e-mails: vpanov@ecko.uran.ru (V.G.P.); varaksin@ecko.uran.ru (A.N.V.)

* Correspondence: bkaznelson@etel.ru; Tel.: +7-343-253-0421; Fax: +7-343-371-7740.

Abstract: Stable suspensions of metal/metalloid oxide nanoparticles (Me-NPs) obtained by laser ablation of 99.99% pure elemental aluminum, titanium or silicon under a layer of deionized water were used separately, or in three binary combinations, or in a ternary combination to induce subchronic intoxications in rats. To this end, the Me-NPs were repeatedly injected intraperitoneally (i.p.) 18 times during 6 weeks before measuring a large number of functional, biochemical, morphological and cytological indices for the organism's status. In many respects, the Al_2O_3-NP was found to be the most toxic species alone and the most dangerous component of the combinations studied. Mathematical modeling with the help of the Response Surface Methodology showed that, as well as in the case of any other binary toxic combinations previously investigated by us, the organism's response to a simultaneous exposure to any two of the Me-NP species under study was characterized by a complex interaction between all possible types of combined toxicity (additivity, subadditivity or superadditivity of unidirectional action and different variants of opposite effects) depending on which outcome a given type was estimated for and on effect and dose levels. With any third MeO-NP species acting in the background, the type of combined toxicity displayed by the other two remained virtually the same or changed significantly, becoming either more or less unfavorable. Various harmful effects produced by the [Al_2O_3-NP+TiO_2-NP+SiO_2-NP]-combination, including its genotoxicity, were substantially attenuated by giving the rats *per os* during the entire exposure period a complex of innocuous bioactive substances expected to increase the organism's antitoxic resistance.

Keywords: nanoparticles; subchronic effects; comparative and combined toxicity; bioprotectors

© 2018 by the author(s). Distributed under a Creative Commons CC BY license.

Preprints (www.preprints.org) | NOT PEER-REVIEWED | Posted: 25 January 2018 doi:10.20944/preprints201801.0238.v1

Peer-reviewed version available at Int. J. Mol. Sci. 2018, 19, 837; doi:10.3390/ijms19030837

Introduction

The toxicity of metal nanoparticles (Me-NPs) and, especially, metal oxide ones (MeO-NPs) has been a subject of extensive studies for our team for the last few years [1-18]. In these endeavors, we have been motivated by the special interest of this class of substances - not so much because it comprises a lot of purposely manufactured ("engineered") NPs as because their analogues are virtually always present in the workplace and ambient air of arc-welding and metallurgical operations, constituting a substantial fraction in the particle size distribution of the polluting condensation aerosols (see examples in [17]). Meanwhile, it is multiple-factor rather than single-agent potentially hazardous nano-impacts on human health that are a common feature of these environments. Thus, the MeO-NP mixture generated by arc-welding and alloyed steel metallurgy usually comprises oxides of iron, manganese, nickel, chrome, vanadium, silicon and other elements. In nonferrous metallurgies, the typical factors are combined exposures to some of the just listed or to some other Me-NPs (e.g. PbO, CuO, and ZnO in copper smelting and refining).

Both the chemical identity of these NPs and quantitative relationships between them vary broadly depending on a specific technology or its phase, the composition of the alloy being molten or welded and welding electrodes being used, the melting temperature, etc. As well as seeking to identify typical patterns and develop further the general theory of combined nano-metal toxicity, our studies therefore aimed to provide specific estimates of it with reference to some actual industrial exposure settings. This explains the choice of the MeO-NP combinations considered in this paper.

Samples of airborne micro- and nano-particles were collected on polycarbonate filters at an aluminum-titanium alloy production facility. The elemental composition of the samples was determined by energy-dispersive analysis with the help of an electron-scanning microscope, AURIGA CrossBeam (Carl Zeiss, Germany). As follows from the averaged data of Table 1, the largest shares belong to three chemical elements: titanium (17.5%), aluminum (14.8%) and silicon (12.0%), which together account for nearly half of the 18 identified elements (disregarding carbon and oxygen since they were components of the filter itself).

Table 1. Averaged Elemental Composition of the Aerosol Particles Collected on Filters from the Workspace Air of Aluminum-Titanium Alloy Production Facilities (as %% of Total Elements Less Carbon and Oxygen).

Element	Percentage content
Al	**14.8**
As	0.1
Ca	8.2
Cl	5.6
Cr	2.5
Cu	0.1
F	1.1
Fe	2.9
K	3.8
Mg	11.4
Na	6.7
Pb	4.0
S	3.6
Si	**12.0**
Sn	0.5
Ti	**17.5**
Zn	5.2
Total	100

Based on these data, we chose TiO_2-NP, SiO_2-NP and Al_2O_3-NP in the form of water suspensions of nanoparticles for experimental assessment of their individual and combined toxicity.

Preprints (www.preprints.org) | NOT PEER-REVIEWED | Posted: 25 January 2018 doi:10.20944/preprints201801.0238.v1

Peer-reviewed version available at Int. J. Mol. Sci. 2018, 19, 837; doi:10.3390/ijms19030837

The first two of the above species belong to the most widely manufactured and used nanomaterials [19] and thus frequently undergo toxicological assessment, though *in vitro* as a rule, and much less often in short-term animal experiments. The scientific literature of this kind dealing with TiO_2-NP toxicity may be exemplified by [20-32], and that on SiO_2-NP toxicity by [33-46] and numerous other sources. We could not find any long-term inhalation exposure studies of these nanomaterials right up to the point when we carried out such an experiment with an industrial aerosol containing a high proportion of nanoscale particles of predominantly amorphous SiO_2 [47]. Apart from several studies performed on unicellular algae or plant cells, the toxicity of Al_2O_3-NPs had been investigated much less, even on cell cultures [48-50], and only one of the latter [50] also involved the administration of a single oral dose to mice. We have failed to find any publication devoted to the comparative and combined toxicity of the three MeO-NP species under consideration or even of any pair of them.

At the same time, it would be of practical importance to find bioprotectors which, if administered in innocuous doses, could enhance the resistance of the organism to the effect of the given combination as it was first done by our team for Ag-NP [7], CuO-NP [10] and for the combinations (NiO-NP+ Mn3O4-NP) [11] or (PbO-NP + ZnO-NP + CuO-NP) [17] (the theoretical and methodological aspects of this line of research have been set out in [51] and [52]). Interestingly, one of the very few studies on nanotoxicity attenuation performed outside our team was concerned with the hepatotoxicity of just TiO_2-NP ameliorated by means of *Cinnamomum cassia* [28].

2. Results and Discussion

2.1. Functional and Biochemical Outcomes of Intoxication

Only 52 out of around 400 values, as follows from Table 2, obtained across all six experimental groups exposed to a one- or two-factor impact were statistically significantly different from the corresponding control values. In relation to comparison of the magnitudes of effect produced by the toxic impact of the various MeO-NP individually, we should make a reservation that due to the technical impossibility of obtaining a stable Al_2O_3 suspension at the concentration of 0.5 mg/mL which was common to our studies (see Section 3), this NP species was administered at half the dose of the other ones (The dose of 0.5 mg per rat was adopted as basic because we had used it in all previous experiments of the same design involving various other MeO-NP). Nevertheless, it is noteworthy that even this dose of Al_2O_3-NP caused virtually the same changes in the majority of the indices as those induced by TiO_2-NP or SiO_2-NP at a twice higher dose, which indirectly points to a greater toxicity of Al_2O_3-NP. Moreover, some of the indices — reduced hemoglobin content, reduced hematocrit, more acidic pH and higher protein, urea, uric acid and creatinine contents of the urine, and a reduced mass coefficient of both kidneys — demonstrated a greater impact of Al_2O_3-NP than that of the other two MeO-NP species (statistically significant in a number of cases).

Table 2. Some Functional and Biochemical Indices of Rat Organism Status after 18 (during 6 Weeks) Intraperitoneal Injections of Suspensions of Various MeO-NP Species Administered Individually or in Binary Combinations (x ± s.e.).

Index	Control	Al_2O_3	TiO_2	SiO_2	Al_2O_3+ TiO_2	Al_2O_3+ SiO_2	TiO_2+ SiO_2
		Group 1	Group 2	Group 3	Group 4	Group 5	Group 6
Initial body mass, g	292.27± 5.02	289.55± 7.93	287.50± 7.40	285.91± 9.17	287.08± 7.29	290.83± 7.53	291.67± 7.47
Final body mass, g	332.27± 7.93	333.18± 7.70	330.46± 9.33	322.27± 8.70	320.00± 3.59	322.50± 5.28	324.17± 7.76
Body mass gain, %	15.13± 1.85	17.30± 2.74	15.66± 1.69	13.14± 2.51	13.41± 2.07	14.70± 1.86	12.58± 2.09

Preprints (www.preprints.org) | NOT PEER-REVIEWED | Posted: 25 January 2018 doi:10.20944/preprints201801.0238.v1

Peer-reviewed version available at Int. J. Mol. Sci. 2018, 19, 837; doi:10.3390/ijms19030837

Number of head-dips into holes during 3 min	4.73± 0.94	2.64± 0.64*	1.92± 0.36*	2.82± 0.64	5.08± 1.02[2]	3.00± 0.59	4.42± 0.67[2]
Number of squares crossed during 3 min	8.18± 1.25	5.82± 1.09	5.67± 0.99	7.00± 0.86	7.58± 1.17	5.00± 0.55*	7.58± 1.19
Temporal summation of sub-threshold impulses, sec,	14.27± 1.29	13.42± 1.19	14.34± 0.99	12.45± 0.91	15.35± 0.85	14.88± 1.08	13.39± 0.86
Left kidney mass, g/100 g body mass	0.30± 0.01	0.28± 0.01	0.30± 0.01[1]	0.30± 0.01[1]	0.30± 0.01[1]	0.29± 0.01	0.30± 0.01
Right kidney mass, g/100 g body mass	0.31± 0.01	0.28± 0.01*	0.30± 0.01[1]	0.30± 0.01[1]	0.30± 0.01[1]	0.30± 0.01[1]	0.30± 0.01
Liver mass, g/100 g body mass	3.08± 0.13	3.14± 0.16	3.08± 0.12	3.08± 0.10	3.22± 0.18	3.22± 0.16	3.19± 0.13
Spleen mass, g/100 g body mass	0.17± 0.01	0.20± 0.01	0.17± 0.01[1]	0.19± 0.01	0.18± 0.01	0.17± 0.01[13]	0.18± 0.01
Left testicle mass, g/100 g body mass	0.55± 0.02	0.52± 0.01	0.53± 0.01	0.55± 0.01	0.55± 0.01	0.55± 0.01	0.53± 0.01
Right testicle mass, g/100 g body mass	0.55± 0.02	0.51± 0.01	0.52± 0.02	0.55± 0.01[1]	0.54± 0.01	0.55± 0.01[1]	0.53± 0.01
Brain mass, g/100 g body mass	0.62± 0.01	0.59± 0.01*	0.58± 0.02*	0.63± 0.01[12]	0.61± 0.01	0.61± 0.01	0.61± 0.01
Hemoglobin, g/L	158.89± 1.16	141.14± 1.99*	149.00± 3.64[1*]	149.71± 2.74[1*]	147.33± 2.87*	146.00± 1.51*	151.25± 2.45*
Erythrocytes, 10^{12} cells/L	7.93± 0.16	7.68± 0.32	7.23± 0.13*	7.58± 0.14	7.61± 0.24	7.48± 0.11*	7.52± 0.10*
Average erythrocyte volume, μm^3	54.69± 0.86	55.05± 0.87	54.29± 0.85	54.34± 0.51	52.17± 0.67[12*]	52.36± 0.57[13*]	54.94± 0.34
Reticulocytes, ‰	13.63± 1.65	25.64± 2.32*	32.60± 3.01*	26.63± 1.66*	29.90± 1.28*	25.86± 1.61*	31.67± 2.73*
Hematocrit, %	21.54± 0.21	19.73± 0.26*	20.21± 0.52*	20.60± 0.40*	20.03± 0.69*	19.59± 0.26*	20.65± 0.28*
Thrombocytes,10^3/µL	847.25± 25.41	860.00± 48.20	910.25± 67.20	857.25± 33.92	831.75± 54.09	926.57± 27.89	880.50± 34.53
Thrombocrit, %	0.23± 0.02	0.26± 0.02	0.28± 0.02	0.26± 0.01	0.24± 0.02	0.27± 0.01	0.25± 0.01
Leukocytes, 10^3/µL	7.20± 0.37	8.98± 0.86*	8.40± 0.43*	7.69± 0.67	9.10± 1.03	9.40± 0.83*	7.85± 0.67
Eosinophils,%	2.20± 0.29	2.88± 0.61	2.38± 0.38	3.25± 0.73	3.13± 0.48	3.57± 0.87	2.13± 0.40
Segmented neutrophils, %	19.50± 0.64	19.88± 1.38	20.63± 1.15	18.88± 1.51	20.00± 0.82	20.43± 1.91	20.50± 0.98
Banded neutrophils, %	1.50± 0.17	1.88± 0.30	0.88± 0.13[1*]	1.88± 0.40[2]	1.00± 0.00[1*]	2.29± 0.29*	1.38± 0.18[2]
Monocytes,%	6.20± 0.39	6.13± 0.61	6.00± 0.53	6.75± 0.49	6.75± 0.49	6.86± 0.34	6.38± 0.42
Lymphocytes,%	70.60±	69.25±	70.13±	69.25±	69.13±	66.71±	69.63±

Preprints (www.preprints.org) | NOT PEER-REVIEWED | Posted: 25 January 2018 doi:10.20944/preprints201801.0238.v1

Peer-reviewed version available at Int. J. Mol. Sci. 2018, 19, 837; doi:10.3390/ijms19030837

	0.95	1.91	1.38	2.27	0.91	2.60	1.13
Succinate dehydrogenase (SDH) in blood lymphocytes, number of formazan granules	589.45 ± 16.55	536.73 ± 17.43*	539.36 ± 16.94*	553.55 ± 17.46	562.67 ± 15.74	551.55 ± 20.54	530.42 ± 16.03*
γ-glutamyl transpeptidase (GGTP), IU/L	2.26± 0.69	1.14± 0.38	1.14± 0.40	1.86± 0.69	2.48± 0.45[12]	3.98± 0.99[1]	0.74± 0.30
Glucose, mol/L	7.09± 0.26	6.80± 0.21	6.33± 0.25*	6.80± 0.30	6.10± 0.30*	6.64± 0.18	7.04± 0.29
Ceruloplasmin in blood serum, mg%	33.14± 1.13	38.09± 1.56*	42.03± 2.05*	40.39± 1.50*	44.06± 1.53[1*]	46.22± 2.35[13*]	42.88± 1.44*
Malonyl dialdehyde (MDA) in blood serum, μmol/L	3.51± 0.49	3.99± 0.19	3.16± 0.28[1]	3.37± 0.31	3.56± 0.48	5.10± 0.37[13*]	4.57± 0.19[23*]
Catalase in blood serum, μmol/L	1.34± 0.25	1.30± 0.22	1.20± 0.27	1.12± 0.22	1.31± 0.22	1.18± 0.24	0.65± 0.12*
Reduced glutathione in whole blood, μmol/L	26.82± 1.19	27.75± 1.36	26.45± 1.18	22.89± 1.841	26.20± 0.87	28.44± 1.473	26.00± 1.39
SH-groups in blood plasma, mmol/L	37.33± 7.38	37.23± 5.67	40.32± 6.88	34.81± 5.11	36.93± 6.04	43.21± 6.99	42.72± 6.90
Total protein content of blood serum, g/L	80.47± 1.42	76.81± 1.97	75.43± 1.40*	75.36± 2.00*	80.49± 2.01	78.20± 1.33	78.93± 2.15
Albumin content of blood serum, g/L	44.34± 0.61	39.49± 0.81*	40.28± 1.35*	40.25± 1.44*	41.31± 1.05*	39.58± 0.67*	40.18± 1.24*
Globulins of blood serum, g/L	36.13± 1.22	37.33± 2.07	35.15± 1.65	35.49± 1.76	39.18± 1.54	38.63± 1.06	38.75± 1.53
A/G index	1.24± 0.04	1.08± 0.06*	1.17± 0.07	1.14± 0.06	1.06± 0.05*	1.03± 0.03*	1.05± 0.05*
AST activity in blood serum, IU/L	218.44± 17.65	257.93± 12.42	261.38± 26.36	193.10± 22.6112	264.61± 25.72	236.81± 17.78	187.39± 5.072
ALT activity in blood serum, IU/L	70.82± 3.24	72.70± 3.10	69.00± 4.19	58.55± 4.281*	66.46± 4.41	66.50± 1.66	63.94± 3.32
De Ritis coefficient	3.12± 0.24	3.57± 0.18	3.75± 0.23	3.31± 0.31	3.76± 0.39	3.55± 0.23	3.01± 0.23
Alkaline phosphatase, IU/L	193.64± 13.08	215.71± 14.74	216.61± 23.36	212.59± 26.36	222.55± 13.71	240.48± 21.89*	236.53± 10.62*
Creatinine in blood serum, μmol/L	36.33± 1.46	33.64± 1.09	30.80± 0.711*	32.40± 1.29*	34.46± 1.71	34.50± 1.49	33.89± 1.352
Bilirubin in blood serum, μmol/L	1.14± 0.13	0.90± 0.15	1.05± 0.15	1.00± 0.10	1.31± 0.13	1.09± 0.14	0.98± 0.14

Preprints (www.preprints.org) | NOT PEER-REVIEWED | Posted: 25 January 2018 doi:10.20944/preprints201801.0238.v1

Peer-reviewed version available at Int. J. Mol. Sci. 2018, 19, 837; doi:10.3390/ijms19030837

Concentration of Ca^{2+} in blood serum, mol/L	2.61± 0.03	2.53± 0.02*	2.54± 0.05	2.55± 0.04	2.56± 0.04	2.57± 0.03	2.52± 0.05
Follicle stimulating hormone in blood serum, IU/L	0.14± 0.02	0.11± 0.00	0.11± 0.01	0.12± 0.01	0.13 ±0.01	0.11 ±0.01	0.11 ±0.01
Luteinizing hormone in blood serum, IU/L	0.13± 0.02	0.14± 0.02	0.24± 0.10	1.31± 0.94	0.94± 0.58	0.35± 0.21	0.77± 0.63
Prolactin in blood serum, IU / L	7.85± 0.62	6.38± 0.58	10.22± 2.59	9.90± 1.91	15.71± 4.51	8.22± 0.82	14.73± 5.25
Testosterone in blood serum, nmol/L	8.20± 3.40	12.50± 3.21	26.51± 9.95	13.26± 5.19	9.77± 2.10	8.45± 4.01	16.28± 4.27
Lactate dehydrogenase (LDH) in blood serum, IU/L	1904.10± 296.03	2402.25± 277.51	2924.38± 530.17	1781.00± 349.35	2208.25± 290.47	2119.50± 305.84	1628.50 ± 149.27
Uric acid in blood serum, μmol/L	120.50± 10.86	154.88± 13.53	135.50± 15.29	128.25± 17.67	121.00± 11.99	122.00± 9.19	115.75± 8.69
Urea in blood serum, mmol/L	4.44± 0.34	3.69± 0.28	3.89± 0.45	3.29± 0.40*	3.59± 0.36	3.71± 0.27	3.73± 0.37
Daily diuresis, mL	29.67± 4.36	21.17± 2.39	26.43± 3.88	28.43± 5.73	33.00± 2.50[1]	24.86± 2.20	31.71± 5.64
Coproporphyrin in urine, nmol/L	162.42± 31.78	135.77± 21.32	120.40± 40.13	185.31± 74.84	135.37± 62.57	111.83± 39.84	155.14± 31.38
Daily coproporphyrin in urine, μmol	8.14± 3.60	6.47± 1.38	5.87± 3.10	3.73± 0.67	4.63± 2.23	5.42± 2.46	5.91± 2.02
δ–ALA in urine, μg/mL	14.11± 3.52	15.63 ±5.08	11.99 ±4.40	10.90 ±4.47	13.87 ±4.37	9.90 ±3.98	12.61 ±2.99
Creatinine in urine, mmol/L	1.57± 0.11	2.56± 0.27*	2.15± 0.35	1.91± 0.161	1.54± 0.141	1.92± 0.131	1.85± 0.17
Endogenous creatinine clearance	1.40± 0.15	1.58± 0.18	1.90± 0.24	1.74± 0.19	1.50± 0.23	1.38± 0.08	1.60± 0.19
Protein in urine, g/L	190.43± 29.63	298.45± 32.35*	216.55± 33.41	180.93± 17.09[1]	196.13± 20.43[1]	193.36± 20.67[1]	211.45± 37.18
Urine pH	7.17± 0.17	6.50± 0.26*	7.33± 0.40	7.36± 0.30	6.79± 0.15	7.00± 0.29	6.93± 0.17
Urea in urine, mmol/L	229.30± 16.00	319.41± 29.85*	278.06± 46.97	240.15± 25.77[1]	211.22± 17.47[1]	262.08± 19.23	238.15± 24.71
Uric acid in urine, μmol/L	234.00± 38.97	319.50± 45.51	292.50± 105.70	304.71± 93.85	204.29± 78.30	201.86± 64.52	213.00± 51.37

The asterisk * designates the values which are statistically significantly different from the respective control ones, and the superscript numbers those statistically significantly different from the corresponding groups denoted with a corresponding number ($p<0.05$ by Student's t-test)

In order to assess for possible combined toxicity, we should consider the group-average values of a given binary exposure group and compare them with the corresponding values of the groups exposed to relevant species individually, performing this comparison in terms of the sign and statistical significance of the differences. Thus, for instance, the group (Al_2O_3-NP + TiO_2-NP) is

Preprints (www.preprints.org) | NOT PEER-REVIEWED | Posted: 25 January 2018 doi:10.20944/preprints201801.0238.v1

Peer-reviewed version available at Int. J. Mol. Sci. 2018, 19, 837; doi:10.3390/ijms19030837

statistically significantly different from the group Al_2O_3-NP in six indices and from the group TiO_2-NP in four indices, which coincide in three cases. Note, in particular, that this combination eliminated the inhibiting effect of the titanium-oxide NPs on the number of head-dips and impacted in the same direction (although not significantly statistically) on the motor activity being simultaneously recorded. It also lifted GGTP activity inhibition caused by each of these MeO-NP species separately. A similar antagonistic effect of the combination follows from the effect of Al_2O_3-NP on the mass of both kidneys and on daily diuresis. At the same time, a statistically significant *enhancement* of the effect produced by Al_2O_3-NP in the combination with TiO_2-NP was deduced from the concentration of ceruloplasmin in the blood serum, whereas for the majority of the toxicodynamic indices the difference being considered was either absent at all or statistically insignificant. Concerning the latter differences, it is, however, of interest to note that the deterioration of the energy metabolism assessed by a statistically significant reduction in the activity of succinate dehydrogenase in blood lymphocytes under exposure to both Al_2O_3-NP and TiO_2-NP administered alone did not actually occur under their combined impact, i.e. we deal with subadditivity (antagonism) of unidirectional action. Note also that, the erythrocyte count being unchanged, the percentage of reticulocytes was substantially and statistically significantly elevated in all experimental groups, particularly under exposure to TiO_2-NP alone or in combination with SiO_2-NP, while the effect was the same in both cases, which suggests subadditivity.

The same Table suggests that a similar effect-dependent ambiguity of the tentative combined toxicity characteristic holds if we compare the actions of the two other combinations with corresponding single-factor impacts. However, the type of action on a certain index may be different for different combinations. Thus, for example, instead of being attenuated, the inhibiting effect on SDH activity in blood lymphocytes in the case of (Al_2O_3-NP + TiO_2-NP) was even more pronounced than that of each of the combination's components individually (with statistically insignificant inter-group differences though). At the same time, the ceruloplasmin-increasing influence of this combination points to the probability of an additive, or even superadditive action. It is not difficult to find similar examples for the indices of combined action of (TiO_2-NP +SiO_2-NP).

As well as in our previous studies, the effect-dependent and dose-dependent ambiguity of the typology of combined binary action was again confirmed by mathematical modeling. Since this experiment is just an additional confirmation of this fundamental postulate justified and repeatedly confirmed previously ([15, 17, 53-55, 57] etc.), we confine ourselves in this paper to illustrating it with a few examples. Thus, comparison of Figures 1 and 2 shows that the combination (SiO_2-NP + TiO_2-NP) displays subadditivity of unidirectional action for one effect (increase in the concentration of ceruloplasmin in the blood serum) and contra-directional action for another one (increase in AST concentration); the combination (SiO_2-NP + Al_2O_3-NP) demonstrates additive and opposite actions, respectively; and the combination (TiO_2-NP + Al_2O_3-NP), additivity and subadditivity of unidirectional action. An example of how the dependence of the type of combined toxicity varies for one and the same effect at different levels of it and different NP doses is illustrated by the isobologram in Figure 3.

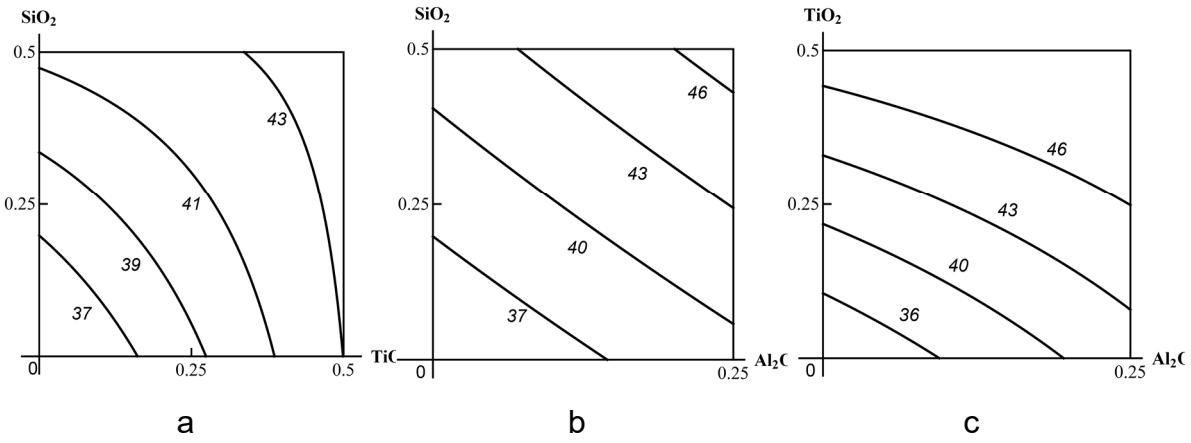

Preprints (www.preprints.org) | NOT PEER-REVIEWED | Posted: 25 January 2018 doi:10.20944/preprints201801.0238.v1

Peer-reviewed version available at Int. J. Mol. Sci. 2018, 19, 837; doi:10.3390/ijms19030837

158 **Figure 1.** Examples of combined subchronic toxicity isobolograms assessed by an increase in the
159 concentration of ceruloplasmin in blood serum under exposure to (a) SiO_2-NP + TiO_2-NP
160 (subadditivity); (b) SiO_2-NP + Al_2O_3-NP (additivity); (c) TiO_2-NP + Al_2O_3-NP (insignificant
161 subadditivity). The axes represent doses of corresponding MeO-NPs in mg per rat; the numbers at
162 the isoboles denote the magnitude of the effect (in mg%). Note that the RSM-model (Response Surface
163 Method) failed to reveal for this effect even the above-mentioned tendency towards superadditivity.

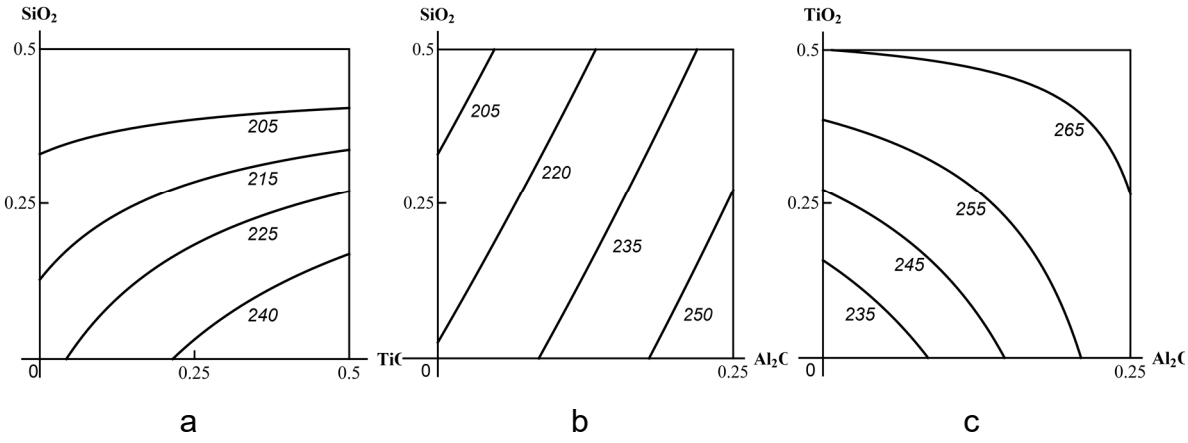

164 **Figure 2.** Examples of combined subchronic toxicity isobolograms assessed by an increase in the
165 concentration of AST in blood serum under exposure to (a) SiO2-NP + TiO2-NP (opposite action); (b)
166 SiO_2-NP + Al_2O_3-NP (opposite action); (c) TiO_2-NP + Al_2O_3-NP (subadditivity of unidirectional action).
167 The axes represent doses of corresponding MeO-NPs in mg per rat; the numbers at the isoboles denote
168 the magnitude of the effect (in IU/L).

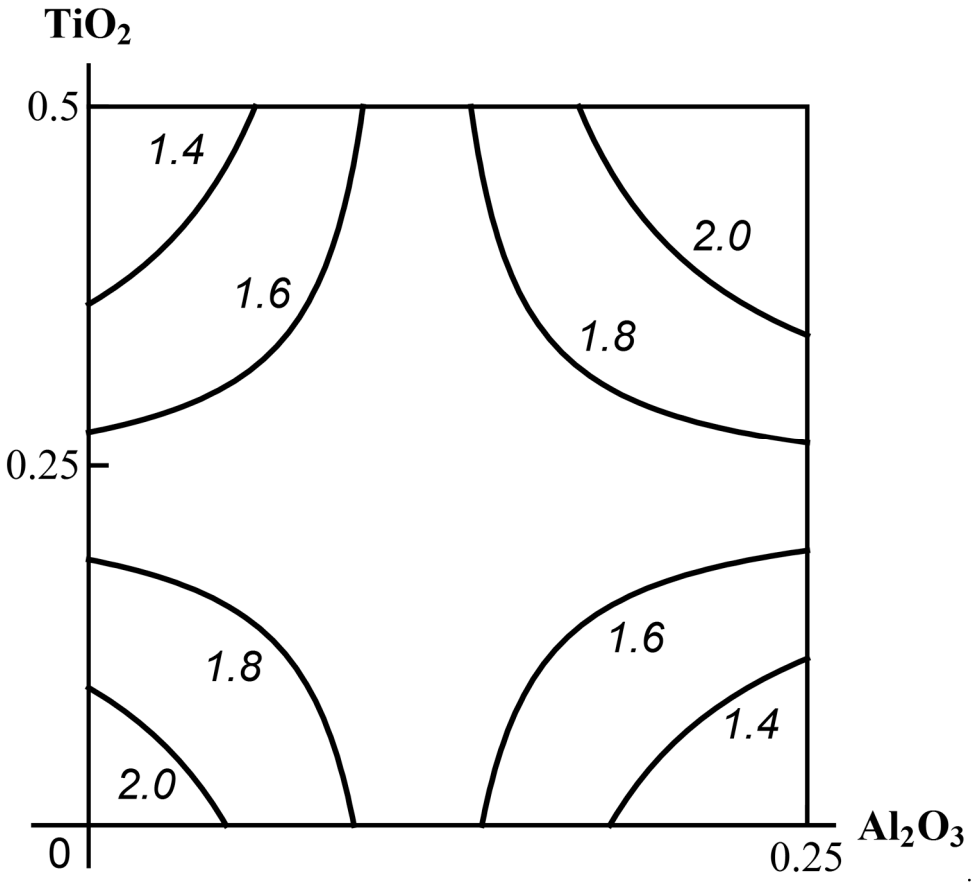

169

170 **Figure 3.** The ambiguity of the TiO_2-NP + Al_2O_3-NP combined subchronic toxicity type assessed by a
171 decrease in the GGTP content of blood serum: subadditivity of unidirectional action at low doses and

Preprints (www.preprints.org) | NOT PEER-REVIEWED | Posted: 25 January 2018 doi:10.20944/preprints201801.0238.v1

Peer-reviewed version available at Int. J. Mol. Sci. 2018, 19, 837; doi:10.3390/ijms19030837

relatively high levels of effect; superadditivity at high doses and similar levels of effect; opposite action at low doses and relatively low levels of effect and also at high doses and relatively low doses of effect. The axes represent doses of corresponding MeO-NPs in mg per rat; the numbers at the isoboles denote the magnitude of the effect (in IU/L).

Table 3 presents once again the values of the binary action indices comparing them with the action of the full ternary combination (Al_2O_3-NP+SiO_2-NP +TiO_2-NP) and the latter with the similar indices in the group exposed to the same ternary combination but simultaneously administered a bioprotective complex (BPC). Besides, the experiment involved a group exposed to the same three MeO-NP species combined at half doses, which was mainly used for constructing a mathematical model with the help of the Response Surface Method (see Section 3). To avoid further complicating the information-laden Table 3, we have not included into it a column of data pertaining to this group. Note, however, that of the seven indices in which the group (Al_2O_3-NP+SiO_2-NP +TiO_2-NP) was statistically significantly different from the controls, dose reduction eliminated the differences for only two of them (reductions in brain mass and GSH content of the blood). To this may be added the normalization of several indices in which the change caused by the combination at full dose was statistically insignificant but sufficiently pronounced (reductions in LDH and urea in blood serum, coproporphyrin in urine, and daily diuresis).

Table 3. Some Functional and Biochemical Indices of Rat Organism Status after 18 (during 6 weeks) Repeated Intraperitoneal Injections of Suspensions of Various MeO-NP Species Administered in Binary and Ternary Combinations (x ± s.e.).

Index	Control	Al_2O_3+ TiO_2	Al_2O_3+ SiO_2	TiO_2+ SiO_2	Al_2O_3+ SiO_2+ TiO_2	Al_2O_3+ SiO_2+ TiO_2 and BPC	BPC
		Group 1	Group 2	Group 3	Group 4	Group 5	Group 6
Initial body mass, g	292.27± 5.02	287.08± 7.29	290.83± 7.53	291.67± 7.47	290.00± 5.56	295.00± 5.16	295.00± 7.03
Final body mass, g	332.27± 7.93	320.00± 3.59	322.50± 5.28	324.17± 7.76	334.55± 8.08	346.50± 4.72	354.50± 7.40
Body mass gain, %	15.13± 1.85	13.41± 2.07	14.70± 1.86	12.58± 2.09	15.40± 2.02	18.34± 2.00	20.32± 1.41*
Number of head-dips into holes during 3 min	4.73± 0.94	5.08± 1.02	3.00± 0.59	4.42± 0.67	3.27± 0.78	3.80± 0.98	4.40± 0.76
Number of squares crossed during 3 min	8.18± 1.25	7.58± 1.17	5.00± 0.55*	7.58± 1.19	6.50± 1.09	4.90± 1.14	7.78± 1.16
Temporal summation of sub-threshold impulses, sec,	14.27± 1.29	15.35± 0.85	14.88± 1.08	13.39± 0.86	14.41± 0.97	13.47± 0.88	11.41± 1.18
Left kidney mass, g/100 g body mass	0.30± 0.01	0.30± 0.01	0.29± 0.01	0.30± 0.01	0.28± 0.01	0.30± 0.01	0.30± 0.01
Right kidney mass, g/100 g body mass	0.31± 0.01	0.30± 0.01	0.30± 0.01	0.30± 0.01	0.29± 0.01	0.30± 0.01	0.30± 0.01
Liver mass, g/100 g body mass	3.08± 0.13	3.22± 0.18	3.22± 0.16	3.19± 0.13	3.09± 0.16	3.04± 0.09	3.21± 0.16
Spleen mass, g/100 g body mass	0.17± 0.01	0.18± 0.01	0.17± 0.01	0.18± 0.01	0.18± 0.01	0.19± 0.00	0.18± 0.01

Preprints (www.preprints.org) | NOT PEER-REVIEWED | Posted: 25 January 2018 doi:10.20944/preprints201801.0238.v1

Peer-reviewed version available at Int. J. Mol. Sci. 2018, 19, 837; doi:10.3390/ijms19030837

Left testicle mass, g/100 g body mass	0.55± 0.02	0.55± 0.01	0.55± 0.01	0.53± 0.01	0.53± 0.02	0.55± 0.02	0.52± 0.01
Right testicle mass, g/100 g body mass	0.55± 0.02	0.54± 0.01	0.55± 0.01	0.53± 0.01	0.53± 0.02	0.55± 0.02	0.52± 0.01
Brain mass, g/100 g body mass	0.62± 0.01	0.61± 0.01	0.61± 0.01	0.61± 0.01	0.59± 0.01*	0.59± 0.01*	0.61± 0.01
Hemoglobin, g/L	158.89± 1.16	147.33± 2.87*	146.00± 1.51*	151.25± 2.45*	147.75± 2.28*	143.26± 1.49*	151.14± 1.92*
Erythrocytes, 10^{12} cells/L	7.93± 0.16	7.61± 0.24	7.48± 0.11*	7.52± 0.10*	7.83± 0.17	7.75± 0.14	7.42± 0.10*
Average erythrocyte volume, μm^3	54.69± 0.86	52.17± 0.67*	52.36± 0.57*	54.94± 0.34[4]	51.73± 0.93*	51.88± 0.82*	56.60± 0.61
Reticulocytes, ‰	13.63± 1.65	29.90± 1.28*[4]	25.86± 1.61*[4]	31.67± 2.73*[4]	15.50± 1.41	26.00± 0.88*[4]	17.67± 4.78
Hematocrit, %	21.54± 0.21	20.03± 0.69*	19.59± 0.26*	20.65± 0.28*	20.20± 0.30*	20.09± 0.45*	21.00± 0.36
Thrombocytes,10^3/µL	847.25± 25.41	831.75± 54.09	926.57± 27.89	880.50± 34.53	882.25± 36.87	979.56± 26.63*[4]	890.25± 36.39
Thrombocrit, %	0.23± 0.02	0.24± 0.02	0.27± 0.01	0.25± 0.01	0.26± 0.01[5]	0.29± 0.01*	0.27± 0.01
Leukocytes, 10^3/µL	7.20± 0.37	9.10± 1.03	9.40± 0.83*	7.85± 0.67	7.78± 0.66	10.04± 0.93*[4]	7.88± 0.46
Eosinophils,%	2.20± 0.29	3.13± 0.48[4]	3.57± 0.87	2.13± 0.40	3.00± 0.42	3.22± 0.36*	3.13± 0.69
Segmented neutrophils, %	19.50± 0.64	20.00± 0.82	20.43± 1.91	20.50± 0.98	20.75± 1.05	20.78± 1.04	18.88± 1.08
Banded neutrophils, %	1.50± 0.17	1.00± 0.00[1*]	2.29± 0.29*	1.38± 0.18[2]	1.63± 0.26	1.67± 0.33	1.25± 0.16
Monocytes,%	6.20± 0.39	6.75± 0.49	6.86± 0.34	6.38± 0.42	6.25± 0.45	6.44± 0.50	6.00± 0.42
Lymphocytes,%	70.60± 0.95	69.13± 0.91	66.71± 2.60	69.63± 1.13	68.50± 1.24	67.89± 0.98	70.75± 1.31
Succinate dehydrogenase (SDH) in blood lymphocytes, number of formazan granules	589.45 ± 16.55	562.67 ± 15.74	551.55 ± 20.54	530.42 ± 16.03*	561.64 ± 15.99	559.50 ± 16.67	578.90 ± 14.48
γ-glutamyl transpeptidase (GGTP), IU/L	2.26± 0.69	2.48± 0.45	3.98± 0.99[4]	0.74± 0.30	1.10± 0.66	1.23± 0.40	1.41± 0.69
Glucose, mol/L	7.09± 0.26	6.10± 0.30*[4]	6.64± 0.18	7.04± 0.29	7.08± 0.18	7.13± 0.35	7.04± 0.17
Ceruloplasmin in blood serum, mg%	33.14± 1.13	44.06± 1.53*	46.22± 2.35*	42.88± 1.44*	42.61± 1.88*	38.36± 2.71	30.54± 1.82
Malonyl dialdehyde (MDA) in blood serum, µmol/L	3.51± 0.49	3.56± 0.48	5.10± 0.37*	4.57± 0.19*	4.28± 0.29	4.20± 0.28	4.09± 0.19

Preprints (www.preprints.org) | NOT PEER-REVIEWED | Posted: 25 January 2018 doi:10.20944/preprints201801.0238.v1

Peer-reviewed version available at Int. J. Mol. Sci. 2018, 19, 837; doi:10.3390/ijms19030837

Catalase in blood serum, μmol/L	1.34± 0.25	1.31± 0.22	1.18± 0.24	0.65± 0.12*	1.10± 0.21	0.74± 0.25	0.86± 0.31
Reduced glutathione in whole blood, μmol/L	26.82± 1.19	26.20± 0.87	28.44± 1.473	26.00± 1.39	22.55± 1.41*43	26.39± 1.364	28.17± 1.35
SH-groups in blood plasma, mmol/L	37.33± 7.38	36.93± 6.04	43.21± 6.99	42.72± 6.90	40.20± 6.66	37.34± 7.64	34.13± 6.64
Total protein content of blood serum, g/L	80.47± 1.42	80.49± 2.01	78.20± 1.33	78.93± 2.15	79.91± 1.82	81.00± 1.79	80.46± 1.59
Albumin content of blood serum, g/L	44.34± 0.61	41.31± 1.05*	39.58± 0.67*	40.18± 1.24*	41.91± 0.88*	43.38± 0.94	44.91± 0.90
Globulins of blood serum, g/L	36.13± 1.22	39.18± 1.54	38.63± 1.06	38.75± 1.53	38.00± 1.40	37.62± 1.45	35.55± 1.30
A/G index	1.24± 0.04	1.06± 0.05*	1.03± 0.03*	1.05± 0.05*	1.11± 0.04*	1.17± 0.05	1.27± 0.05
AST activity in blood serum, IU/L	218.44± 17.65	264.61± 25.72	236.81± 17.78	187.39± 5.072	213.91± 17.83	214.32± 18.45	205.88± 10.52
ALT activity in blood serum, IU/L	70.82± 3.24	66.46± 4.41	66.50± 1.66	63.94± 3.32	66.75± 3.55	83.09± 5.13*4	84.98± 4.69
De Ritis coefficient	3.12± 0.24	3.76± 0.39	3.55± 0.23	3.01± 0.23	3.22± 0.25	2.67± 0.31	2.50± 0.24
Alkaline phosphatase, IU/L	193.64± 13.08	222.55± 13.71	240.48± 21.89*	236.53± 10.62*	200.30± 12.154	209.78± 21.48	261.99± 24.46*
Creatinine in blood serum, μmol/L	36.33± 1.46	34.46± 1.71	34.50± 1.49	33.89± 1.352	35.39± 1.03	34.39± 1.25	34.54± 0.94
Bilirubin in blood serum, μmol/L	1.14± 0.13	1.31± 0.13	1.09± 0.14	0.98± 0.14	1.10± 0.16	1.06± 0.08	0.99± 0.17
Concentration of Ca^{2+} in blood serum, mol/L	2.61± 0.03	2.56± 0.04	2.57± 0.03	2.52± 0.05	2.58± 0.02	2.66± 0.06	2.68± 0.05
Follicle stimulating hormone in blood serum, IU/L	0,14± 0,02	0,13± 0,01	0,11± 0,01	0,11± 0,01	0.14± 0.01	0.14± 0.01	0.14± 0.01
Luteinizing hormone in blood serum, IU/L	0.13± 0.02	0.94± 0.58	0.35± 0.21	0.77± 0.63	0.12± 0.01	0.16± 0.02	0.15± 0.01
Prolactin in blood serum, IU / L	7,85± 0,62	15,71± 4,51	8,22 0,82	14,73± 5,25	6.84± 0.35	8.42± 0.86	7.52± 0.46
Testosterone in blood serum, nmol/L	8,20± 3,40	9,77± 2,10	8,45± 4,01	16,28± 4,27	13.34± 8.17	13.47± 7.99	8.41± 2.58
Lactate dehydrogenase (LDH) in blood serum, IU/L	1904.10± 296.03	2208.25± 290.47	2119.50± 305.84	1628.50± 149.27	1709.88± 246.58	1313.22± 259.49	1433.00± 179.78

Preprints (www.preprints.org) | NOT PEER-REVIEWED | Posted: 25 January 2018 doi:10.20944/preprints201801.0238.v1

Peer-reviewed version available at Int. J. Mol. Sci. 2018, 19, 837; doi:10.3390/ijms19030837

Uric acid in blood serum, μmol/L	120.50± 10.86	121.00± 11.99	122.00± 9.19	115.75± 8.69	123.63± 9.61	128.89± 12.32	127.75± 11.33
Urea in blood serum, mmol/L	4.44± 0.34	3.59± 0.36	3.71± 0.27	3.73± 0.37	3.35± 0.42	4.93± 0.45[4]	4.49± 0.42
Daily diuresis, mL	29.67± 4.36	33.00± 2.50	24.86± 2.20	31.71± 5.64	26.86± 4.14	29.00± 6.52	32.40± 8.36
Coproporphyrin in urine, nmol/L	162.42± 31.78	135.37± 62.57	111.83± 39.84	155.14± 31.38	76.11± 24.08	176.13± 49.92	79.15± 26.76
Daily coproporphyrin in urine, μmol	8.14± 3.60	4.63± 2.23	5.42± 2.46	5.91± 2.02	4.34± 2.23	13.97± 6.94	2.76± 1.30
δ–ALA in urine, μg/mL	14.11± 3.52	13.87± 4.37	9.90± 3.98	12.61± 2.99	13.48± 5.22	13.21± 3.28	8.31± 1.84
Creatinine in urine, mmol/L	1.57± 0.11	1.54± 0.14[4]	1.92± 0.13	1.85± 0.17	2.03± 0.19	1.74± 0.25	1.43± 0.21
Endogenous creatinine clearance	1.40± 0.15	1.50± 0.23	1.38± 0.08	1.60± 0.19	1.49± 0.19	1.46± 0.18	1.50± 0.13
Protein in urine, g/L	190.43± 29.63	196.13± 20.431	193.36± 20.671	211.45± 37.18	233.13± 30.83	354.33± 66.07	243.93± 22.83*
Urine pH	7.17± 0.17	6.79± 0.15	7.00± 0.29	6.93± 0.17	6.93± 0.37	7.75± 0.25	7.500± 0.000
Urea in urine, mmol/L	229.30± 16.00	211.22± 17.47[4]	262.08± 19.23	238.15± 24.71	289.74± 28.72	242.70± 39.98	222.15± 16.29
Uric acid in urine, μmol/L	234.00± 38.97	204.29± 78.30	201.86± 64.52	213.00± 51.37	216.00± 52.97	287.17± 109.69	209.00± 43.27

The asterisk * designates the values which are statistically significantly different from the control ones, and the superscript numbers mark the values which are statistically significantly different from the corresponding values of the groups denoted with a corresponding number ($p<0.05$ by Student's t-test)

Thus, the toxic impact of the ternary combination assessed by shifts in the functional and biochemical indices of the organism's status was not only insubstantial but did not demonstrate any clear dependence on dose as well. Moreover, there were almost no statistically significant distinctions from the same indices in the three groups of binary exposures. In advance of further discussion, we may note that the analysis of some other unfavorable indices presented below has given in all respects an essentially different picture.

It should be noted, however, that characterizing the type of combined toxic impact, ambiguous even for binary combinations, proves to be extremely complicated where three factors are involved. For solving this problem, we had previously proposed [59] and then re-used [16] a two-phase risk-oriented analysis. At the first phase, we estimate all variants of combined toxicity for each of the three pairs of toxics involved in the ternary combination. At the second phase of analysis, all toxic exposure effects are classified depending on whether the type of combined toxicity displayed by one and the same pair with a third factor added is found to be more unfavorable for the organism (class A), less unfavorable for the organism (class B) or remains essentially unchanged (class C). Prior to carrying out such analyses, we defined criteria of such classification [59].

All previously conducted experiments with three-factor combinations of soluble salts or metal-oxide nanoparticles provided satisfactory stability of this classification, i.e. it was fully or partly reproducible in all cases where we considered as a third (background) factor one by one all components of the three-factor combination. Examples of effects falling into various classes based on the data of the current experiment are presented as isobolograms in Figures 4–6.

Preprints (www.preprints.org) | NOT PEER-REVIEWED | Posted: 25 January 2018 doi:10.20944/preprints201801.0238.v1

Peer-reviewed version available at Int. J. Mol. Sci. 2018, 19, 837; doi:10.3390/ijms19030837

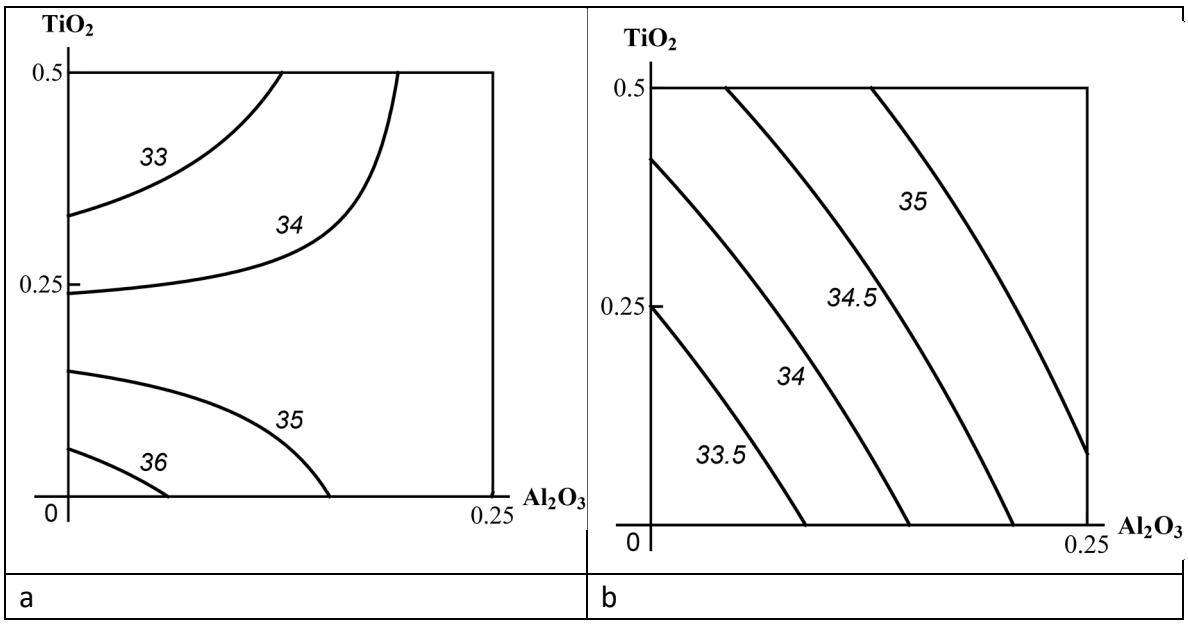

Figure 4. An example of three-factor toxicity falling into class "A": (a) a subadditive or opposite action (for different levels of effect and doses) of the combination (Al_2O_3-NP.+ TiO_2-NP) in the absence of a third factor on the creatinine content of blood serum transforms (for all effect levels and doses) into (b) an additive one in the presence of simultaneously influencing SiO_2-NPs. Me-NP doses are plotted on the axes in mg per rat. The numbers at the lines correspond to the magnitude of the effect (μmol/L).

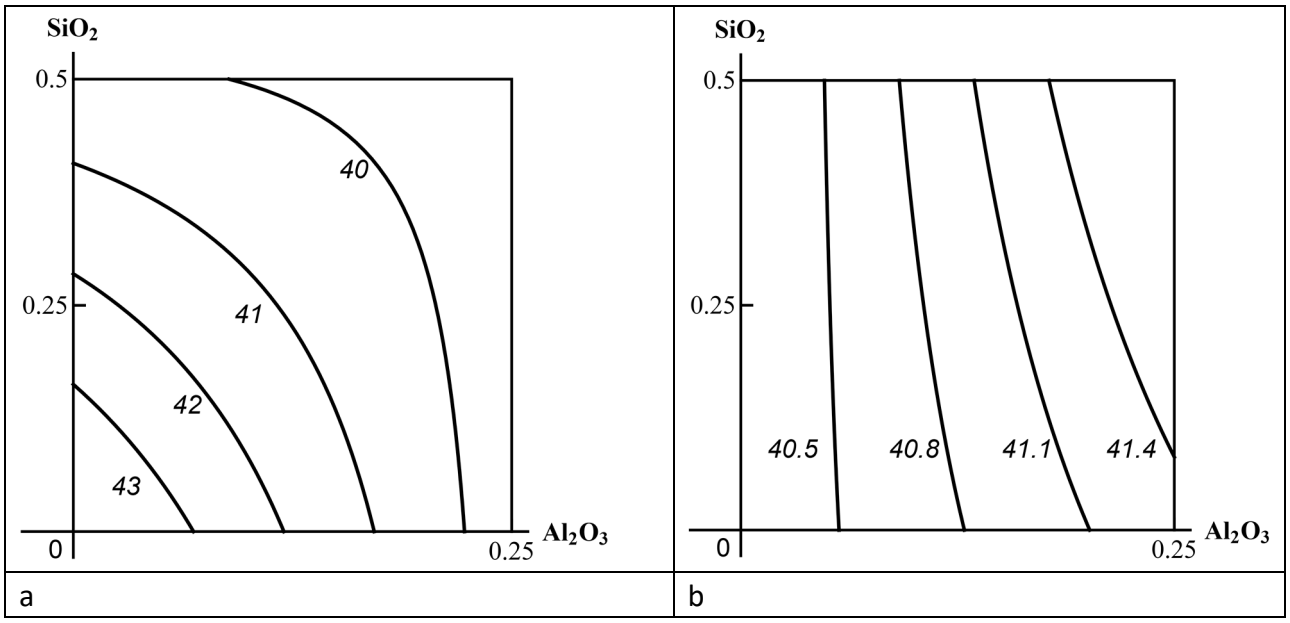

Figure 5 An example of three-factor toxicity falling into class "B": (a) a unidirectional (subadditive) action of SiO_2-NP + Al_2O_3-NP in the absence of a third factor on the albumin content of blood serum transforms into (b) a single-factor action of Al_2O_3-NP alone in the presence of simultaneously influencing TiO_2-NPs. The numbers at the lines correspond to the magnitude of the effect (g/L).

Preprints (www.preprints.org) | NOT PEER-REVIEWED | Posted: 25 January 2018 doi:10.20944/preprints201801.0238.v1

Peer-reviewed version available at Int. J. Mol. Sci. 2018, 19, 837; doi:10.3390/ijms19030837

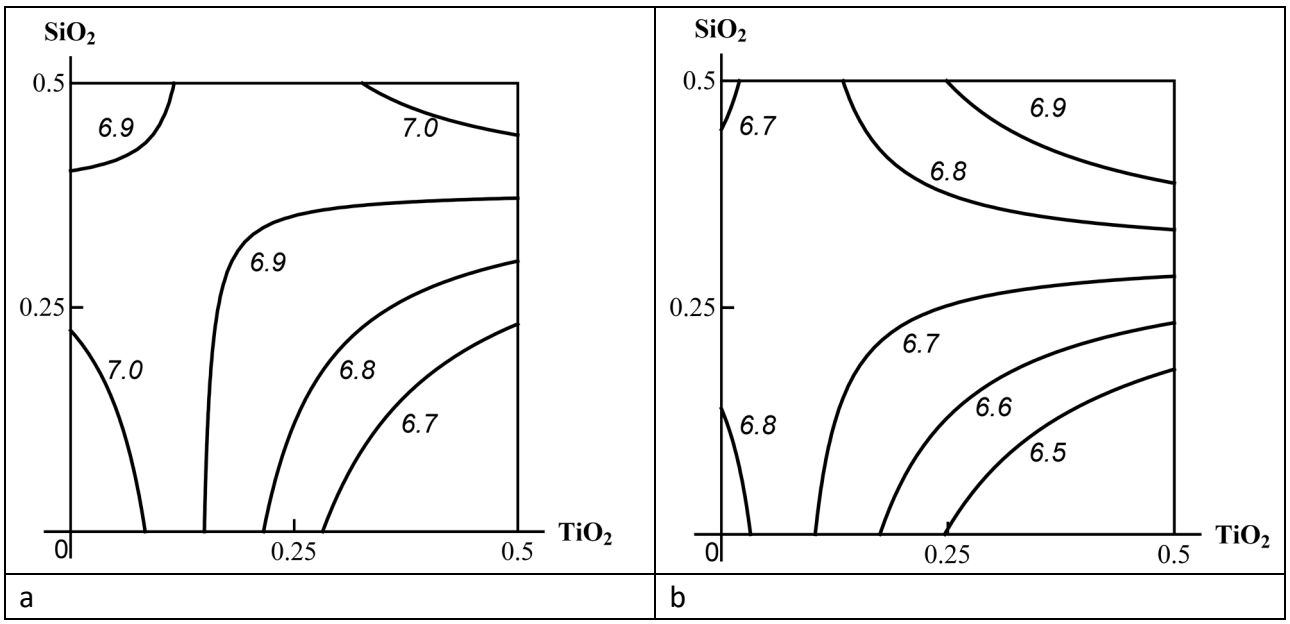

Figure 6. An example of three-factor toxicity falling into class "C": the isoboles of combined action of SiO_2-NP + TiO_2-NP on the glucose content of blood serum virtually fully match (a) in the absence of a third factor and (b) in the presence of Al_2O_3-NP. The MeO-NP doses are plotted on the axes in mg per rat. The numbers at the lines correspond to the magnitude of the effect (μmol/L).

On the whole, among all the effects of toxic impact presented in Table 3 and classified reliably (totally 150, allowing for all variants of considering one of the factors as a background third one), class A accounted for 35%, class B for 43%, and class C for 22%. Where Al_2O_3-NP was the third factor, class A (42%) prevailed to some extent, whereas in the case of the other two MeO-NP species class B did (44%).

2.2. Morphometry of the Most Characteristic Histological Changes in Kidneys and Liver

Similar two approaches (common-sense based comparison of group-average values and mathematical modeling based on the Response Surface Method) were also used for assessing the comparative and combined toxicity of the MeO-NPs under study by morphometric indices of NP-caused damage to internal organs, in particular to kidneys and liver. As well as in all previously investigated subchronic intoxications with metal-containing nanoparticles, the most pronounced histopathological manifestation of renal toxicity was degenerative changes in the epithelium of the proximal convoluted tubules, including brush border loss, and, ultimately, complete epithelial desquamation. As can be seen from Table 4, both indices were somewhat higher for the impact of TiO_2-NP compared not only with that of Al_2O_3-NP (which could be explained by the lower dosage of the latter) but also with the impact of SiO_2-NP. Most likely, the metals impact directly on the kidneys not so much as persistent MeO-NP as in the form of ions released by them as a result of solubilization in biological milieus, which has been repeatedly proven by us (e.g. [15,17]). We may therefore assume that the special nephrotoxicity of TiO_2-NP is explained just by its highest *in vivo* solubility, which we modeled by adding fetal bovine serum (FBS) *in vitro* to each of the nano-suspensions (Figure 7).

Table 4. Morphometric Indices of Damage to the Epithelium of the Proximal Convoluted Tubules in Rat Kidneys after Subchronic Exposure to Al_2O_3-NP, TiO_2-NP and SiO_2-NP Individually or in Binary Combinations (x±s.e.).

Index	Group exposed i.p. to MeO-NP						
	Control	Al_2O_3	TiO_2	SiO_2	Al_2O_3 + TiO_2	Al_2O_3 + SiO_2	TiO_2 + SiO_2

Preprints (www.preprints.org) | NOT PEER-REVIEWED | Posted: 25 January 2018 doi:10.20944/preprints201801.0238.v1

Peer-reviewed version available at Int. J. Mol. Sci. 2018, 19, 837; doi:10.3390/ijms19030837

Brush border loss, %	1.49 ± 0.56	1.85 ± 0.47	3.61 ± 0.99*	2.24 ± 0.58	6.45 ± 1.07*x@	4.23 ± 0.80*+@	3.64 ± 0.70*
Epithelial desquamation, %	0.00 ± 0.00	0.15 ± 0.15	0.42 ± 0.36	0.30 ± 0.25	0.97 ± 0.48*	0.29 ± 0.17	0.14 ± 0.14

Statistically significant (P<0.05 by Student's t-test) difference: * from the control value, x from the value of the group administered SiO_2, x from the value of the group administered TiO_2, @ from the value of the group administered Al_2O_3

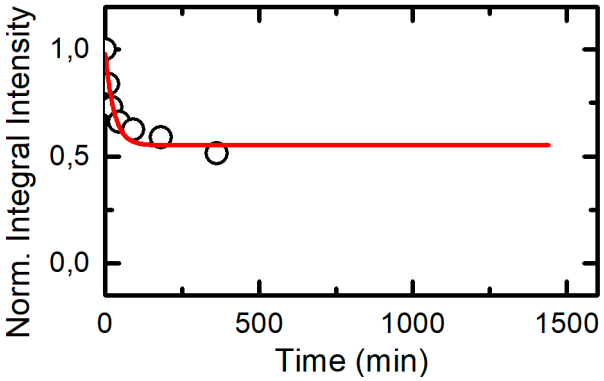

Al_2O_3-NP

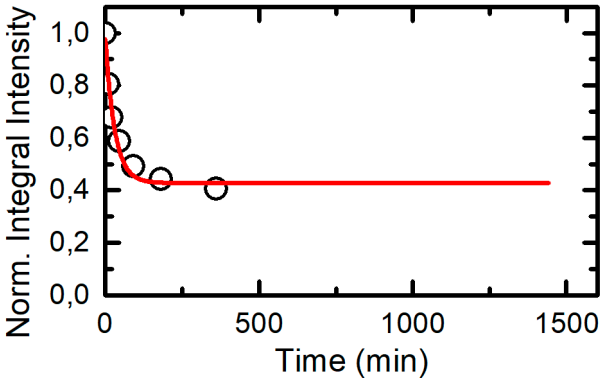

TiO_2-NP

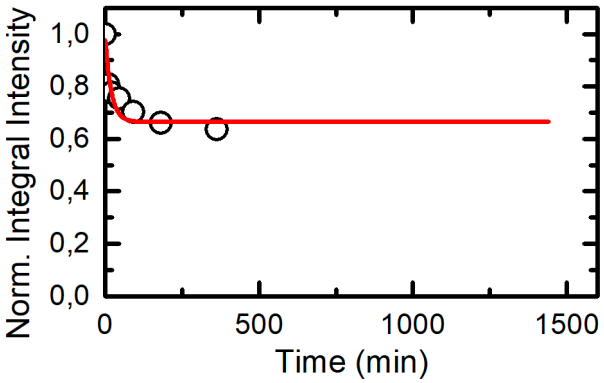

SiO_2-NP

Figure 7. The kinetics of nanoparticle dissolution in suspension upon addition of FBS.

It is easy to note that both indices under the effect of each of the binary combinations including Al_2O_3-NP are higher than the corresponding values under an individual exposure to the second component of the combination, which was not actually observed for the combination (TiO_2-NP + SiO_2-NP). We could take as a measure of nephrotoxic effect the difference between the values of the

Preprints (www.preprints.org) | NOT PEER-REVIEWED | Posted: 25 January 2018 doi:10.20944/preprints201801.0238.v1

Peer-reviewed version available at Int. J. Mol. Sci. 2018, 19, 837; doi:10.3390/ijms19030837

corresponding index in the exposed and control groups. For the index of brush border loss, this difference is equal to 0.36 for Al_2O_3-NP, 2.12 for TiO_2-NP, and 0.75 for SiO_2-NP. Thus, the expected value of this difference upon full summation of the effects in the combination (Al_2O_3-NP + TiO_2-NP) could have been equal to 2.48, but in reality we obtained 4.96; to 1.11 and 2.74 for (Al_2O_3-NP + SiO_2-NP), respectively; and to 2.87 and 2.15 for (TiO_2-NP + SiO_2-NP). Whereas in the latter case the impression is of an actually additive or slightly subadditive action, in the former two it appears to be more of a superadditive one. In the combination (Al_2O_3-NP + TiO_2-NP), for which the second morphometric nephrotoxicity index was statistically significant, a similar tentative calculation also points to superadditivity.

Table 5 reproduces the same morphometric nephrotoxicity indices for the binary combinations in comparison with the corresponding indices of the ternary one (for full and half doses of each of the MeO-NP species in its composition). We may also note that the addition of SiO_2-NP to the most nephrotoxic combination (Al_2O_3-NP + TiO_2-NP) strengthened the effect but insignificantly (possible subadditivity of action), while the addition of Al_2O_3-NP to the combination (SiO_2-NP + TiO_2-NP) doubled it making it statistically significant, though for brush border loss only. Thus, as well as in the above analysis of functional and biochemical effects, the impression again is one of a leading role of Al_2O_3-NP (even at a relatively low dose) in the development of combined toxicity due to the MeO-NP species considered, although the most toxic exposure factor for kidneys proved to be (TiO_2-NP) alone.

The relationship of this effect with the impact of the combination under study is confirmed by its explicit dependence on the dose of the whole combination (Table 5). At the same time, by way of preempting Subsection 2.5, let us note that the background administration of the bioprotective complex appears to have reduced the nephrotoxic effect of the ternary combination to a much greater extent than the halving of the dose.

Going back to the tentative calculations carried out above based on the data of Table 4, we can see that the summary gain in the brush border loss index due to the effect of the three factors, compared with the control value, was equal to 3.23, while being equal to 5.70 under the actual combined impact of these factors, which again points to a likely prevalence of superadditive action. Similar summation of the values of the second nephrotoxicity effect (% epithelial desquamation) provides the expected value of 0.87 for the sum of three individual exposures and 1.04 for the actual combined exposure, which also suggests superaddivity.

Table 5. Morphometric Indices of Damage to the Epithelium of the Proximal Convoluted Tubules in Rat Kidneys after Subchronic Exposure to Al_2O_3-NP, TiO_2-NP and SiO_2-NP Individually or in Binary Combinations (x±s.e.).

Index	Group receiving i.p. MeO-NP						
	Control	Al_2O_3 + TiO_2	Al_2O_3 + SiO_2	TiO_2+ SiO_2	Al_2O_3 + TiO_2+ SiO_2 at half dose	Al_2O_3 + TiO_2+ SiO_2 in full doses	Al_2O_3 + TiO_2+ SiO_2 in full doses with BPC
Brush border loss, %	1.49 ± 0.56	6.45 ± 1.07*	4.23 ± 0.80*	3.64 ± 0.70*#	3.06 ± 0.84#	7.19 ± 1.47*	1.99 ± 0.43#
Epithelial desquamation, %	0.00 ± 0.00	0.97 ± 0.48*	0.29 ± 0.17	0.14 ± 0.14	0.66 ± 0.47	1.04 ± 0.39*	0.18 ± 0.16#…

Statistically significant (P<0.05 by Student's t-test) difference * from control value, # from the value of the group administered the ternary combination in full dose without BPC.

Using RSM-modeling (Response Surface Method) again for predicting the type of combined nephrotoxicity outside the range of experimentally tested doses, we, on the whole, received support for the above tentative estimates. Indeed, as follows from the isobologram in Figure 8, only two Al_2O_3-

Preprints (www.preprints.org) | NOT PEER-REVIEWED | Posted: 25 January 2018 doi:10.20944/preprints201801.0238.v1

Peer-reviewed version available at Int. J. Mol. Sci. 2018, 19, 837; doi:10.3390/ijms19030837

NP-including binary combinations reveal a definite additivity of the nephrotoxic action as judged by brush border loss with an insignificant, though clear departure from it towards synergism (superadditivity). On the contrary, the effect of the combination (SiO_2-NP + TiO_2-NP) is clearly dominated by the contribution of TiO_2-NP, and it is only at minimal doses of the latter that we can see additivity or some subadditivity of the SiO_2-NP action). Some type of antagonism (i.e. subadditivity or opposite action) in this combination is clearly prevalent in the index of epithelial desquamation as well (Figure 9)

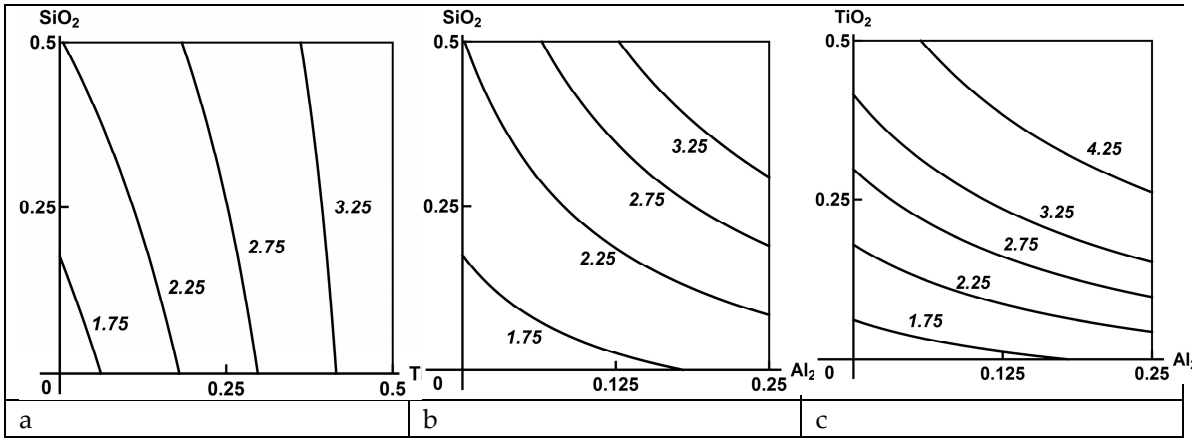

Figure 8. Isobolograms of combined subchronic toxicity assessed by brush border loss in the epithelium of kidney tubules: (a) SiO_2-NP + TiO_2-NP (single-factor effect of TiO_2-NP with insignificant additivity); (b) SiO_2-NP + Al_2O_3-NP (additivity tending towards synergism); (c) TiO_2-NP + Al_2O_3-NP (the same type of action). The axes represent doses of corresponding MeO-NPs in mg per rat. The numbers at the isoboles denote the magnitude of the effect (as %%).

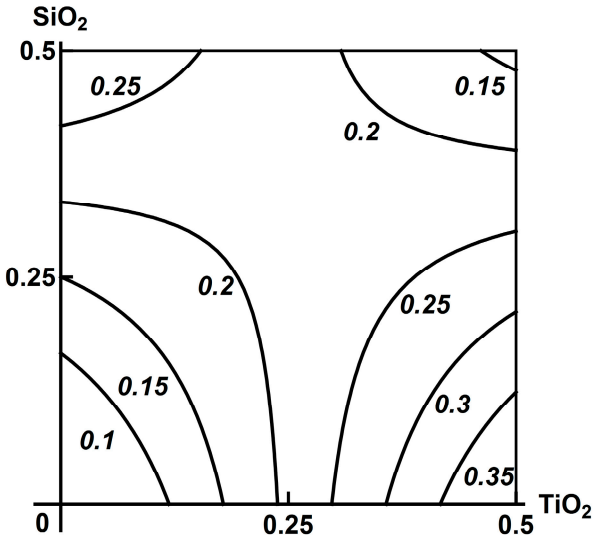

Figure 9. Isobologram of combined subchronic toxicity of SiO_2-NP + TiO_2-NP assessed by kidney tubule epithelium desquamation: subadditivity of unidirectional action at lower doses of both MeO-NPs, superadditivity at maximum doses of both species, different variants of opposite action in combinations of low doses of one MeO-NP with high doses of the other. The axes represent doses of corresponding MeO-NPs in mg per rat; the numbers at the isoboles denote the magnitude of the effect (as %%).

At the same time, for these morphometric nephrotoxicity indices as well the type of combined binary action may change more or less substantially under the influence of the third component of the combination, which is exemplified by Figure 10.

Preprints (www.preprints.org) | NOT PEER-REVIEWED | Posted: 25 January 2018 doi:10.20944/preprints201801.0238.v1

Peer-reviewed version available at Int. J. Mol. Sci. 2018, 19, 837; doi:10.3390/ijms19030837

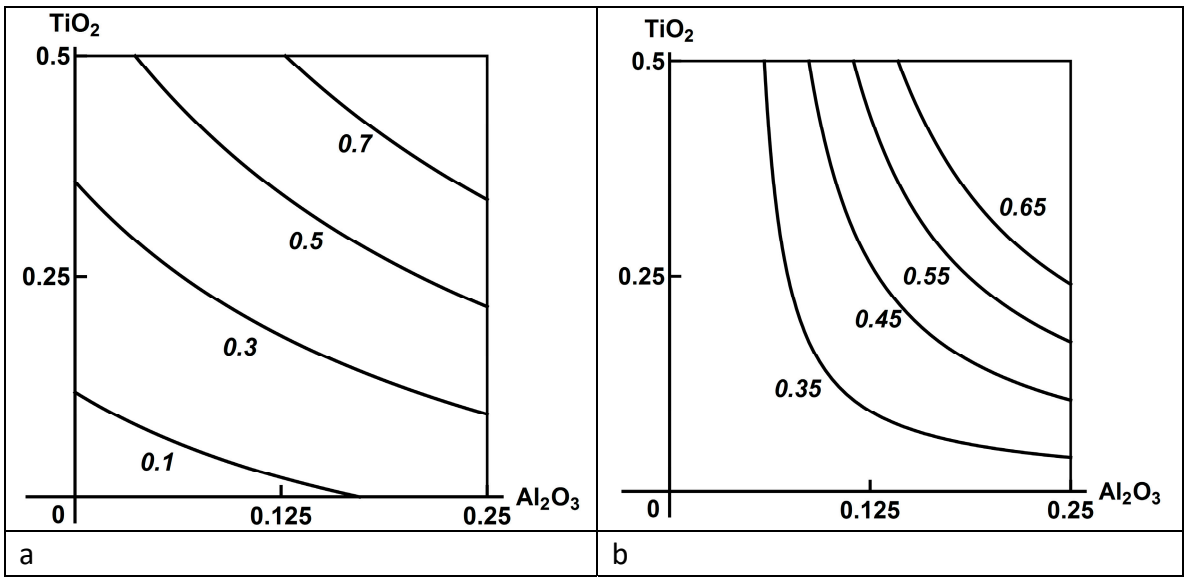

Figure 10. Isoboles of combined subchronic toxicity of Al_2O_3-NP + TiO_2-NP assessed by epithelial desquamation of kidney tubules: (a) additivity of unidirectional action in the absence of a third MeO-NP, (b) superadditivity in the presence of SiO_2-NP (an example of a three-factor action falling within class A). The axes represent doses of corresponding MeO-NPs in mg per rat; the numbers at the isoboles denote the magnitude of the effect (as %%).

As well as in all our previous subchronic experiments with MeO-NPs without exception, the histological liver preparations displayed enhanced degeneration of the hepatocytes up to an increase in the number of cells which have lost their nuclei. As can be seen from Tables 6 and 7, this quantitative index was increased in all exposure groups of this experiment too. Previously, we saw nearly as often a decrease in the proportion of binuclear hepatocytes providing evidence of suppression of reparative proliferation, and this effect was observed in this case as well. The number of Kupffer cells was, on the contrary, increased statistically significantly in all groups, though not that much. Whether the latter shift was associated only with the activation of this population of resident macrophages under the effect of nanoparticles engulfed by them or is an indirect sign of enhanced apoptosis of hepatocytes (considering the role of Kupffer cells in the utilization of apoptotic bodies [60]) is a matter for discussion but, in either case, we had invariably observed it in our previous experiments with other MeO-NPs or Me-NPs. The fact that all these effects were least pronounced in the group of individual exposure to Al_2O_3-NP is likely to be explained by the same lowest dose.

Table 6. Morphometric Indices of Liver Status in Rats after Subchronic Exposure to Al_2O_3-NP, TiO_2-NP and SiO_2-NP Individually or in Binary Combinations (x±s.e.).

Number of cells of a given type per 100	Group receiving i.p. MeO-NP						
	Control	Al_2O_3	TiO_2	SiO_2	Al_2O_3 + TiO_2	Al_2O_3 + SiO_2	TiO_2 + SiO_2
Acaryotic hepatocytes	10.30 ± 1.09	17.60 ± 0.98*	41.27 ± 1.36*	39.67 ± 2.58*	29.45 ±1.47*	41.88 ± 1.72*	41.90 ± 1.48*
Binucleated hepatocytes	6.65 ± 0.83	5.67 ± 0.55	4.13 ± 0.47*	3.27 ± 0.46*	5.13 ± 0.46	3.13 ± 0.37*	3.75 ± 0.52*
Kupffer cells	14.28 ± 0.45	18.07 ± 0.62*	21.43 ± 0.68*	21.03 ± 0.62*	19.58 ± 0.60*	18.80 ± 0.72*	21.05 ± 0.53*

Note: the sign * denotes a statistically significant (P<0.05 by Student's t-test) difference from the corresponding control value. Also, there is a statistically significant difference: (1) in all indices, between the group exposed to Al_2O_3-NP and the group of individual exposure to the other two MeO-NPs; (2) in the number of akaryotic hepatocytes, between the group exposed to (Al_2O_3-NP + TiO_2-NP) and the groups of exposure to both components individually; between the group exposed to (Al_2O_3-

Preprints (www.preprints.org) | NOT PEER-REVIEWED | Posted: 25 January 2018 doi:10.20944/preprints201801.0238.v1

Peer-reviewed version available at Int. J. Mol. Sci. 2018, 19, 837; doi:10.3390/ijms19030837

NP + SiO_2-NP) and the group of exposure to Al_2O_3-NP alone; between the group exposed to (Al_2O_3-NP + TiO_2-NP) and the group of exposure to Al_2O_3-NP alone; (3) in the number of binucleated hepatocytes, between the group exposed to (Al_2O_3-NP + SiO_2-NP) and the group of exposure to Al_2O_3-NP alone; (4) in the number of Kupffer cells, between the group exposed to (Al_2O_3-NP + TiO_2-NP) and the group of exposure to TiO_2-NP alone; between the group exposed to (Al_2O_3-NP + SiO_2-NP) and the group of exposure to SiO_2-NP alone.

Comparison of the binary exposure groups with the groups exposed to corresponding two components individually (Table 6), and with the group exposed to the full ternary combination (Table 7) gives the impression of subadditivity as a predominant type of combined hepatotoxicity of the MeO-NPs under consideration, which was again confirmed by RSM-modeling. In this paper, we confine ourselves to illustrating the latter statement with two isobolograms in Figure 11, which demonstrate simultaneously that in this case as well the introduction of a third component may change the type of combined action displayed by the other two, including towards greater adversity for the organism (class A). Note also that halving the dose of the ternary combination attenuated the hepatotoxic effect only in its direct morphometric indicator (i.e. the number of akaryotic hepatocytes).

Table 7. Morphometric Indices of Liver Status in Rats after Subchronic Exposure to Al_2O_3-NP, TiO_2-NP and SiO_2-NP in Binary or Ternary Combination (x±s.e.).

Number of cells of a given type per 100	Group receiving i.p. MeO-NP						
	Control	Al_2O_3 + TiO_2	Al_2O_3 + SiO_2	TiO_2+ SiO_2	Al_2O_3 + TiO_2+ SiO_2 at half dose	Al_2O_3 + TiO_2+ SiO_2 в in full dose	Al_2O_3 + TiO_2+ SiO_2 in full dose with BPC
Akaryotic hepatocytes	10.30 ± 1.09	29.45 ±1.47*	41.88 ± 1.72*#	41.90 ± 1.48*#	16.92 ± 0.81 *#	31.85 ± 1.74*	27.13 ± 1.20*#
Binucleated hepatocytes	6.65 ± 0.83	5.13 ± 0.46	3.13 ± 0.37*	3.75 ± 0.52*	5.00 ± 0.33*	4.05 ± 0.78*	3.35 ± 0.32*
Kupffer cells	14.28 ± 0.45	19.58 ± 0.60*	18.80 ± 0.72*	21.05 ± 0.53*	20.58 ± 0.48*	20.08 ± 0.75*	18.58 ± 0.53*

Note: the sign * denotes a statistically significant (P<0.05 by Student's t-test) difference from control value, # from the index of the group administered the ternary combination in full dose without BPC.

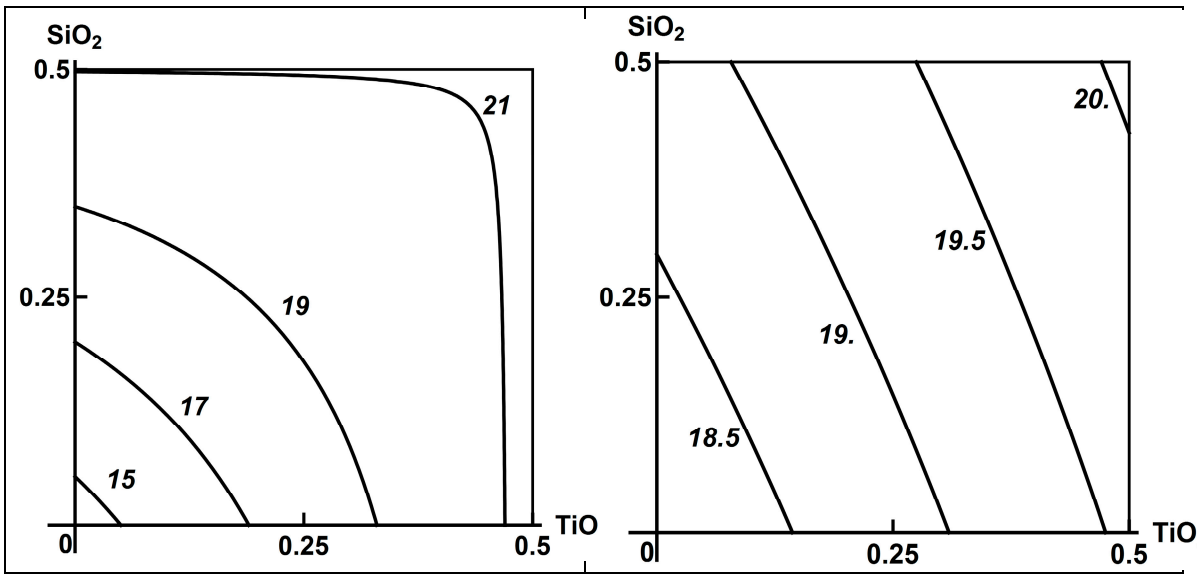

Figure 11. Isobolograms of combined subchronic toxicity of SiO_2-NP + TiO_2-NP assessed by an increase in the number of Kupffer cells: (a) subadditivity of unidirectional action in the absence of a

Preprints (www.preprints.org) | NOT PEER-REVIEWED | Posted: 25 January 2018 doi:10.20944/preprints201801.0238.v1

Peer-reviewed version available at Int. J. Mol. Sci. 2018, 19, 837; doi:10.3390/ijms19030837

third MeO-NP, (b) additivity in the presence of Al_2O_3-NP (an example of three-factor effect falling within class A). The axes represent doses of corresponding MeO-NPs in mg per rat; the numbers at the isoboles denote the magnitude of the effect (as %%).

2.3. Cytological Analysis of Tissue Imprints of Some Organs

In this experiment, we assessed, for the first time, damage to the cells of various organs in rats under subchronic nano-intoxication (single- and two-factor exposures) not only *in situ* on histological preparations but also by cytological analysis of tissue touch preparations (imprints).

Noteworthy is a certain essential similarity between the estimates obtained by this method with estimates commonly obtained in histological preparation morphometry. Indeed, the signs of hepatotoxicity typical of the action of practically all Me-NP species studied in our experiments — an increase in the proportion of degenerated hepatocytes with an increase or decrease in the percentage of binucleated hepatocytes, as well as an increase in the proportion of Kupffer cells — proved to be essential to a certain extent (with few exceptions) judging by the cytological data as well, both under an exposure to Al_2O_3-NP, SiO_2-NP or TiO_2–NP individually and in response to any binary combination of these factors (Table 8). Of additional interest is the increase (statistically significant mostly) in the percentage of neutrophils and eosinophils found under all these exposures, which points to an inflammatory response of hyperergic type. Given the fact that the Al_2O_3-NP dose was half the dose of the other two MeO-NPs, the impression is that Al_2O_3-NPs are the most hepatotoxic, thus enhancing the hepatotoxicity of the combinations. However, the inter-group differences are far from being unambiguous, making them unhelpful for judging about the nature of the combined action.

Table 8. Some Cytological Characteristics of Rat Liver Tissue Imprints as a Percentage of Total Cell Count in Rats after Subchronic Exposure to Al_2O_3-NP, TiO_2-NP and SiO_2-NP Individually or in Binary Combinations (x±s.e.).

Factor	Duct epithelial cells	Degenerated hepatocytes	Binucleated hepatocytes	Kupffer cells	Neutrophils	Eosinophils
Al_2O_3-NP	10.51± 1.79	9.49± 1.71	0.68± 0.48	6.10± 1.39*	10.17± 1.76*	3.73± 1.10
TiO_2-NP	9.52± 1.71*	8.16± 1.60	0.68± 0.48	2.38± 0.89	8.50± 1.63*	5.10± 1.28*
SiO_2-NP	14.29± 2.04	5.78± 1.36	1.36± 0.68	3.74± 1.11	8.16± 1.60*	5.10± 1.28*
Al_2O_3-NP + TiO_2-NP	12.71± 1.95	11.34± 1.86*	1.03± 0.59	4.81± 1.25	5.84± 1.37	2.06± 0.83
Al_2O_3+ SiO_2-NP	11.90± 1.89	8.16± 1.60	1.02± 0.59	5.44± 1.32*	6.80± 1.47	5.10± 1.28*
TiO_2+ SiO_2-NP	11.41± 1.84	9.73± 1.72	0.67± 0.47	4.36± 1.18	9.73± 1.72*	4.36± 1.18*
Control	14.86± 2.07	6.42± 1.42	1.01± 0.58	2.03± 0.82	3.72± 1.10	1.35± 0.67

Note: The asterisk * denotes values which are statistically significantly different from the control ($P<0.05$ by Student's t-test).

In principle, the same applies to the cytology of the kidney tissue imprints (Table 9). Note only that as well as in the histological examination, damage was observed predominantly in the cells of proximal (rather than distal) convoluted tubules, and the fact of toxic inflammation in this organ is evidenced by a largely eosinophilic reaction. In one case only, comparison of a binary action with a single-factor one seems to point to a statistically significant antagonism in the combination TiO_2+ SiO_2.

Preprints (www.preprints.org) | NOT PEER-REVIEWED | Posted: 25 January 2018 doi:10.20944/preprints201801.0238.v1

Peer-reviewed version available at Int. J. Mol. Sci. 2018, 19, 837; doi:10.3390/ijms19030837

Table 9. Some Cytological Characteristics of Kidney Tissue Imprints as a Percentage of Total Cell Count in Rats after Subchronic Exposure to Al_2O_3-NP, TiO_2-NP and SiO_2-NP Individually or in Binary Combinations (x±s.e.).

Factor	Proximal tubule cells	Degenerated cells of proximal tubules	Distal tubule cells	Degenerated cells of distal tubules	Neutrophils	Eosinophils
Al_2O_3-NP	60.33± 2.82	13.00± 1.94	7.00± 1.47	8.33± 1.60	4.33± 1.18	2.33± 0.87
TiO_2-NP	56.00± 2.87*	14.00± 2.00	7.67± 1.54	8.33± 1.60	5.00± 1.26	5.00± 1.26*
SiO_2-NP	56.67± 2.86*	14.67± 2.04	9.00± 1.65	6.00± 1.37	5.67± 1.33	2.00± 0.81
Al_2O_3-NP + TiO_2-NP	58.67± 2.84*	16.33± 2.13*	8.00± 1.57	5.67± 1.33	4.00± 1.13	2.67± 0.93
Al_2O_3+ SiO_2-NP	56.67± 2.86*	16.00± 2.12*	7.00± 1.47	9.00± 1.65	4.00± 1.13	2.67± 0.93
TiO_2+ SiO_2-NP	57.48± 2.85*	14.29± 2.02	9.30± 1.67	7.64± 1.53	4.65± 1.21	1.66± 0.74+
Control	67.67± 2.70	10.00± 1.73	7.67± 1.54	5.00± 1.26	5.00± 1.26	0.67± 0.47

Note: The asterisk * denotes values which are statistically significantly different from the control; the sign + denotes the difference from the group administered TiO_2-NP alone ($P<0.05$ by Student's t-test).

In the tissue imprints of both mesenteric lymph nodes (Table 10) and spleen (Table 11), conspicuous is a reduction in the percentage of lymphocytes with an increase in the percentage of other cell elements, mainly inflammatory cells. In the lymph node imprints, the total mature lymphocyte and prolymphocyte counts in the group (Al_2O_3+ SiO_2) are significantly less than in the Al_2O_3 group and insignificantly greater than in the SiO_2 group. This is likely to point to subadditivity of toxic action, but in the other index (percentage of macrophages) that gave a statistically significant difference of the group (Al_2O_3+ SiO_2) from each of the single-factor exposure groups, the sign of this difference is the same (additivity supposedly). The action of the combination (Al_2O_3+ TiO_2) also appears to be significantly additive according to the second index and subadditive according to the first one. In the spleen imprints, possible additivity of action in the combination (Al_2O_3+ SiO_2) is suggested just by a unidirectional change in the percentage of lymphocytes.

Table 10. Some Cytological Characteristics of Mesenteric Tissue Imprints as a Percentage of Total Cell Count in Rats after Subchronic Exposure to Al_2O_3-NP, TiO_2-NP and SiO_2-NP Individually or in Binary Combinations (x±s.e.).

Factor	Mature lymphocytes and prolymphocytes	Lymphoblasts	Reticular cells	Plasmocytes	Macrophages	Neutrophils	Eosinophils
Al_2O_3-NP	85.33± 2.04*	2.67± 0.93	1.33± 0.66	3.33± 1.04	2.67± 0.93	1.33± 0.66	3.33± 1.04
TiO_2-NP	85.33± 2.04*	2.67± 0.93	1.67± 0.74	3.33± 1.04	4.00± 1.13	1.33± 0.66	1.67± 0.74
SiO_2-NP	74.67± 2.51*	3.00± 0.98	1.33± 0.66	9.00± 1.65*	3.33± 1.04	0.33± 0.33	8.33± 1.60*
Al_2O_3-NP + TiO_2-NP	82.00± 2.72*	1.50± 0.86	1.50± 0.86	6.00± 1.68*	3.50± 1.30	1.50± 0.86	4.00± 1.39

Preprints (www.preprints.org) | NOT PEER-REVIEWED | Posted: 25 January 2018 doi:10.20944/preprints201801.0238.v1

Peer-reviewed version available at Int. J. Mol. Sci. 2018, 19, 837; doi:10.3390/ijms19030837

Al_2O_3+ SiO_2-NP	82.89± 2.18*+	1.34± 0.67	0.67± 0.47	3.02± 0.99+	7.05± 1.48*@+	1.34± 0.67	3.69± 1.09+
TiO_2+ SiO_2-NP	81.40± 2.24*+	1.66± 0.74	1.33± 0.66	3.32± 1.03+	6.98± 1.47*+	1.99± 0.81	3.32± 1.03+
Control	90.67± 1.68	1.67± 0.74	1.00± 0.57	2.00± 0.81	1.67± 0.74	1.33± 0.66	1.67± 0.74

Note: The asterisk * denotes values which are statistically significantly different from the control; the sign @ denotes the difference from the group administered TiO_2-NP alone; the sign + the difference from the group administered SiO_2-NP alone ($P<0.05$ by Student's t-test).

Table 11. Some Cytological Characteristics of Spleen Tissue Imprints as a Percentage of Total Cell Count in Rats after Subchronic Exposure to Al_2O_3-NP, TiO_2-NP and SiO_2-NP Individually or in Binary Combinations (x±s.e.).

Factor	Lymphocytes	Lymphoblasts	Reticular cells	Plasmocytes	Macrophages	Neutrophils	Eosinophils
Al_2O_3-NP	76.00± 2.47*	1.00± 0.57	1.00± 0.57	3.00± 0.98	5.00± 1.26	7.00± 1.47*	7.00± 1.47
TiO_2-NP	75.08± 2.49*	0.66± 0.47	0.66± 0.47	1.66± 0.74	4.65± 1.21	7.64± 1.53*	9.63± 1.70*
SiO_2-NP	78.67± 2.37*	0.33± 0.33	1.00± 0.57	1.00± 0.57	3.67± 1.09	5.67± 1.33	9.67± 1.71*
Al_2O_3-NP + TiO_2-NP	82.67± 2.19+@	1.00± 0.57	0.67± 0.47	1.00± 0.57	3.67± 1.09	4.00± 1.13	7.00± 1.47
Al_2O_3+ SiO_2-NP	79.33± 2.34*	0.33± 0.33	0.67± 0.47	1.00± 0.57	4.67± 1.22	8.33± 1.60*	5.67± 1.33
TiO_2+ SiO_2-NP	78.67± 2.37*	1.00± 0.57	0.67± 0.47	1.33± 0.66	2.33± 0.87	8.33± 1.60*	7.67± 1.54*
Control	87.00± 1.94	0.67± 0.47	1.33± 0.66	1.67± 0.74	3.00± 0.98	2.67± 0.93	3.67± 1.09

Note: The asterisk * denotes values which are statistically significantly different from the control; the sign @ denotes the difference from the group administered TiO_2-NP alone; the sign + the difference from the group administered Al_2O_3-NP alone ($P<0.05$ by Student's t-test).

Thus, even a descriptive analysis of the tissue imprint cytology data again points to a probable ambiguity of combined toxicity type for various organs and cells. This tentative statement was confirmed by RSM-based mathematical modeling, typical examples of which are represented by several isoboles obtained for two combinations: Al_2O_3-NP+SiO_2-NP (Figure 12) and Al_2O_3-NP+TiO_2-NP (Figure 13).

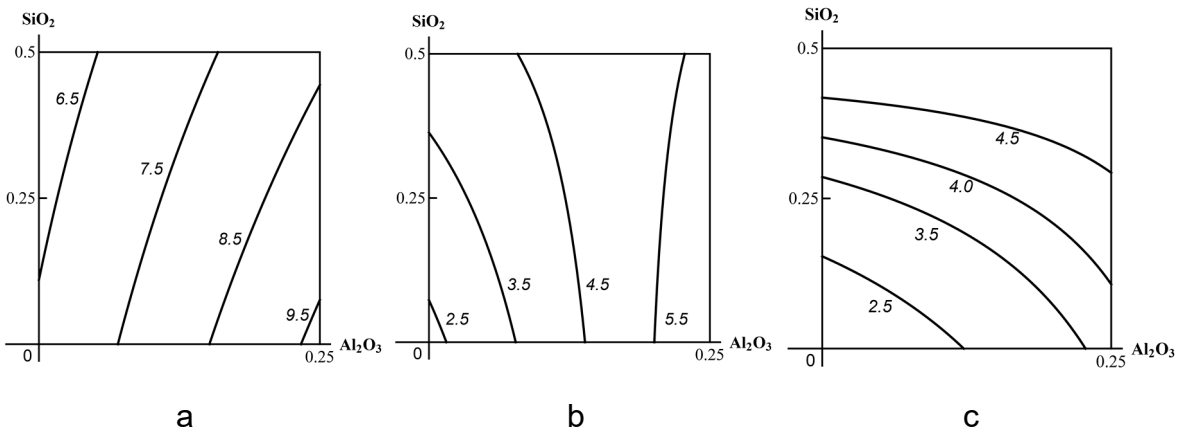

Preprints (www.preprints.org) | NOT PEER-REVIEWED | Posted: 25 January 2018 doi:10.20944/preprints201801.0238.v1

Peer-reviewed version available at Int. J. Mol. Sci. 2018, 19, 837; doi:10.3390/ijms19030837

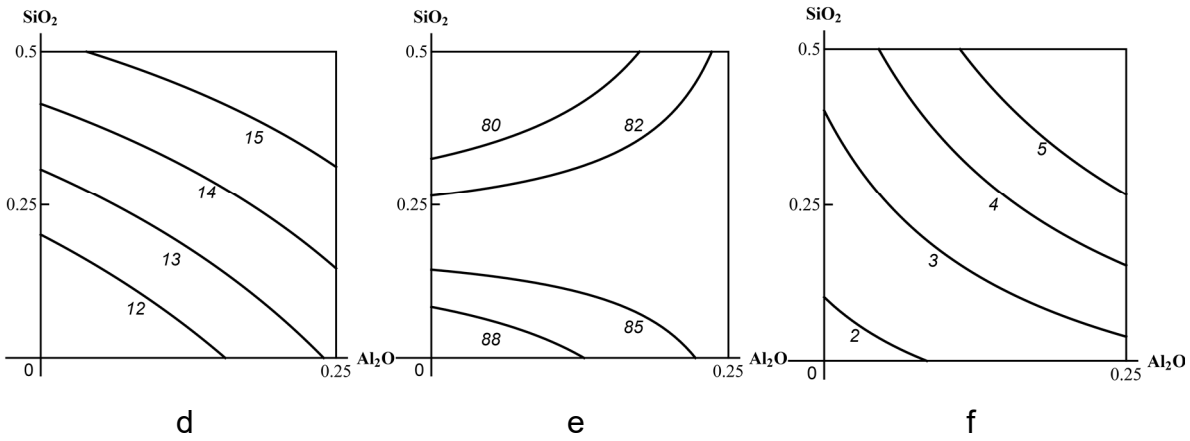

Figure 12. Examples of isobolograms of combined subchronic toxicity of Al_2O_3-NP+SiO_2-NP assessed by: (a) impact on the percentage of degenerated hepatocytes in the liver tissue imprint (unidirectional action); (b) impact on the percentage of Kupffer cells in the same imprint (additivity of unidirectional action at low doses of Al_2O_3-NP transient to a single-factor action at higher doses); (c) impact on the percentage of eosinophils in the same imprint (subadditivity of unidirectional action); (d) impact on the percentage of degenerated epithelial cells of proximal kidney tubules in the kidney tissue imprint (additivity of unidirectional action); (e) impact on the percentage of mature lymphocytes and prolymphocytes in the mesenteric lymph node tissue imprint (subadditivity of unidirectional action at low doses of SiO_2-NP transient to opposite action at higher doses); (e) impact on the percentage of macrophages in the same imprint (superadditivity of unidirectional action). The axes represent doses of SiO_2-NP and Al_2O_3-NP in mg per rat; the numbers at the isoboles denote the magnitude of the effect (as %%).

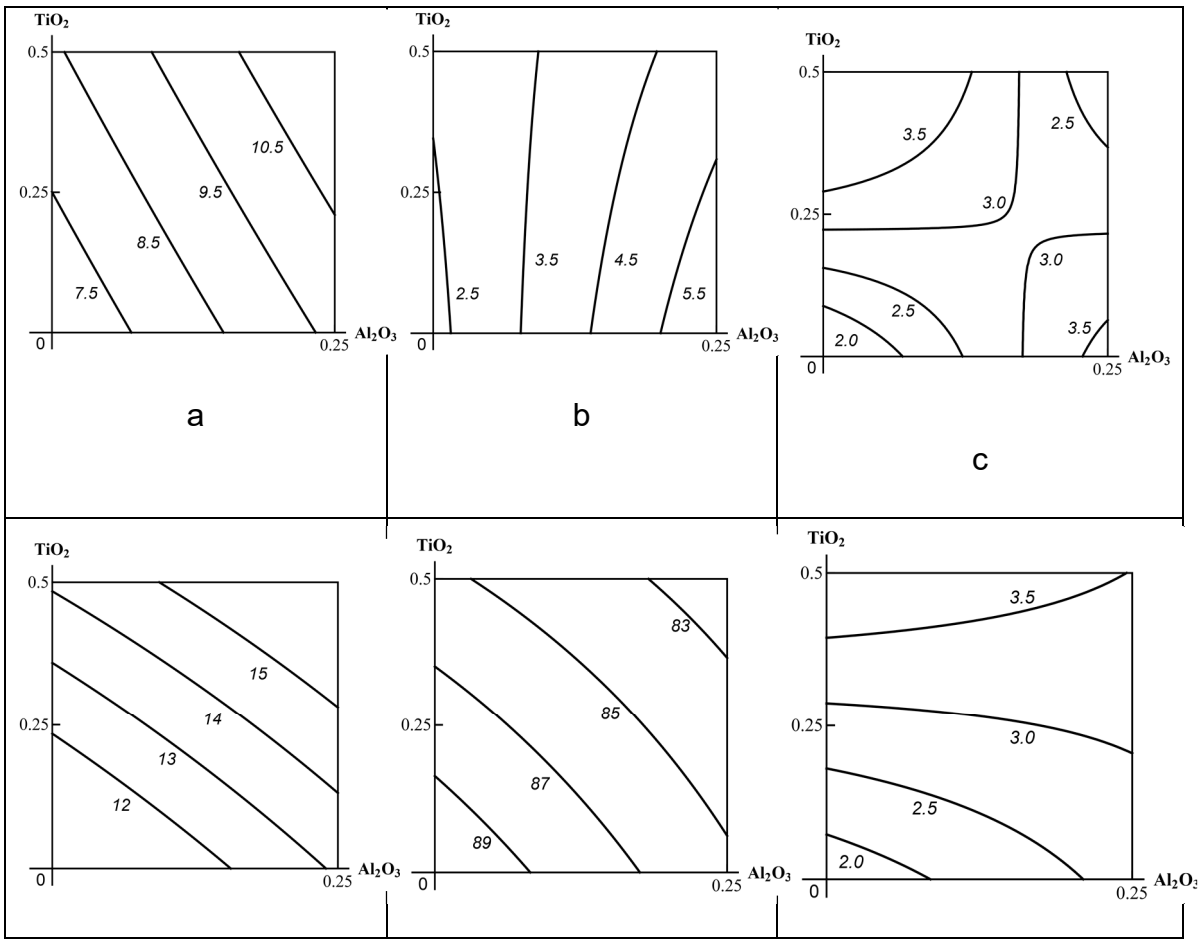

Preprints (www.preprints.org) | NOT PEER-REVIEWED | Posted: 25 January 2018 doi:10.20944/preprints201801.0238.v1

Peer-reviewed version available at Int. J. Mol. Sci. 2018, 19, 837; doi:10.3390/ijms19030837

d	e	f

Figure 13. Examples of isoboles of combined subchronic toxicity of Al_2O_3-NP+TiO_2-NP assessed by: (a) impact on the percentage of degenerated hepatocytes in the liver tissue imprint (additivity of unidirectional action); (b) impact on the percentage of Kupffer cells in the same imprint (single-factor action); (c) impact on the percentage of eosinophils in the same imprint (subadditivity of unidirectional action at low doses and relatively high levels of effect; superadditivity at high doses and low levels of effect; opposite action at high doses of one of the toxicants and relatively high levels of effect);(d) impact on the percentage of degenerated cells in the epithelium of the proximal tubules in the kidney tissue imprint (additivity of unidirectional action); (e) impact on the percentage of mature lymphocytes and prolymphocytes in the mesenteric lymph node tissue imprint (additivity); (f) impact on the percentage of macrophages in the same imprint (largely additive unidirectional action with transformation into an opposite one). The axes represent corresponding doses of TiO_2-NP and Al_2O_3-NP in mg per rat; the numbers at the isobole denote the magnitude of the effect (в %%).

A similar typological variety of combined action judging according to the cytological indices may also be demonstrated for the third binary combination (TiO_2-NP+SiO_2-NP), but for the sake of reducing the volume of this paper we do not provide corresponding isoboles. Note only that we have intentionally chosen for comparison one and the same set of toxic action effects from two different binary combinations in order to illustrate the possibility of both mismatch and match between the types of combined toxicity in relation to a certain effect, even where these pairs differed in one factor only. Thus, for instance, the action of the pair (Al_2O_3-NP+SiO_2-NP) on the percentage of degenerated hepatocytes proved to be opposite while that of the pair (Al_2O_3-NP+TiO_2-NP) was additive. At the same time, both combinations had an additive action on the percentage of degenerated tubular epithelium cells.

2.4. Genotoxic Effect

The genotoxic effect of the nanoparticles that we had studied previously *in vivo* was assessed by the «fragmentation coefficient» (C_{fr}) in an RAPD assay on a genomic DNA isolated from cells of various organs and tissues. In a number of studies we have found that the genotoxicity of nanoparticles of silver and gold [7], manganese and nickel oxides [11], and copper, lead and zinc oxides [10, 16] is *polyorganic*. Although the extent of increase in C_{fr} may be different for different organs (depending, supposedly, on the intensity of cell proliferation and on the degree of toxic damage to cells), the *comparative* genotoxicity of different NPs independent of organ was found to be unambiguous as a rule. To reduce effort and cost, we therefore thought it possible to confine ourselves to conducting RAPD testing on one kind of cells of the whole organism, namely nucleated cells of circulating blood.

The results of this testing, performed using a similar experimental model of subchronic intoxication, are presented in Table 12. We can see that all three MeO-NPs provided a statistically significant genotoxic effect. That this effect is associated with the toxic exposure is evidenced by the dependence of the effect on the level of exposure (dose). Indeed, whereas the ternary combination of nanoparticles in full dose caused a 1.6 times increase in C_{fr} compared with the control value, the half dose of it brought about an increase of 1.2 times only ($P<0.05$). Indirect evidence of a causal relationship between this effect and the polysystemic toxic impact of the substances under consideration is the fact that, as well as according to a number of the above integral, morphometric and cytological indices of the impact, the genotoxicity of the nanoparticles studied diminishes in the sequence Al_2O_3-NP >> TiO_2-NP ≥ SiO_2-NP. (Note again that the higher effect of Al_2O_3-NP compared with SiO_2-NP and TiO_2-NP appears to be especially noteworthy given the fact that the dose of the latter was one half as high). This rank agreement between systemic toxicity and genotoxicity is not surprising as the former is based on cytotoxicity, the primary mechanisms of which include, in common with those of DNA damage, free radical and sorption interactions of the nanoparticle surface and of metal ions released from it with membranes and bio-macromolecules.

Preprints (www.preprints.org) | NOT PEER-REVIEWED | Posted: 25 January 2018 doi:10.20944/preprints201801.0238.v1

Peer-reviewed version available at Int. J. Mol. Sci. 2018, 19, 837; doi:10.3390/ijms19030837

As follows from the same Table 12, the genotoxic effect of all three *binary combinations* is, to a degree, higher (though not always statistically significantly) than that of MeO-NP species acting alone, the presence of Al_2O_3-NP in the combination being of greatest importance in this respect as well.

Table 12. Increase in the Coefficient of Genomic DNA Fragmentation (C_{fr}) (as per RAPD Test) of Nucleated Blood Cells in Rats after 18 (during 6 Weeks) Repeated Intraperitoneal Injections of Suspensions of Various MeO-NPs Individually and in Binary or Ternary Combination (x ± s.e.).

	C_{fr}
Al_2O_3-NP	$0.4470+0.0038^{*+x}$
TiO_2-NP	$0.4328+0.00548^{*}$
SiO_2-NP	$0.4288+0.0061^{*}$
Al_2O_3-NP +TiO_2-NP	$0.5416+0.0046^{*@}$
Al_2O_3-NP +SiO_2-NP	$0.4872+0.0041^{*x@}$
TiO_2-NP+SiO_2-NP	$0.4391+0.0061^{*+x}$
Al_2O_3-NP+TiO_2-NP+SiO_2-NP (half doses)	$0.4849+0.0068^{*+x@}$
Al_2O_3-NP +TiO_2-NP+SiO_2-NP (full doses)	$0.6430+0.0189^{*+x@}$
Al_2O_3-NP +TiO_2-NP+SiO_2-NP+BPC	$0.4742+0.0067^{*+x@}$
BPC	0.4143+0.0047
Control	0.4023+0.0064

Note: The signs denote values differing statistically significantly ($P<0.05$ by Student's t-test) as follows: * from the control value, $^{+}$ from the value under exposure to TiO_2-NP, ^{x} from the value under exposure to SiO_2-NP, $^{@}$ from the value under exposure to SiO_2-NP. Also, there is a statistically significant difference between the groups administered the ternary MeO-NP combination in full and half doses, and in full dose and in the same dose with background administration of the BPC.

If we consider as a measure of genotoxic effect the difference between the values of C_{fr} in each of the exposed and control group, one gets the impression that this effect is superadditive in the Al_2O_3-NP-containing binary combinations (especially with TiO_2-NP), as well as in the full ternary combination, while in the binary combination (TiO_2-NP + SiO_2-NP) it is rather subadditive. To ascertain what type of combined action we are dealing with we again resorted to RSM-modeling.

As follows from the corresponding isoboles (Figure 14), subadditivity does manifest itself across the entire range of doses and responses for the pair (SiO_2-NP + TiO_2-NP), whereas for the pair (TiO_2-NP + Al_2O_3-NP) there is undoubted superadditivity, which for the pair (SiO_2-NP + Al_2O_3-NP) reveals itself just as a slightly noticeable (and statistically insignificant) departure from additivity.

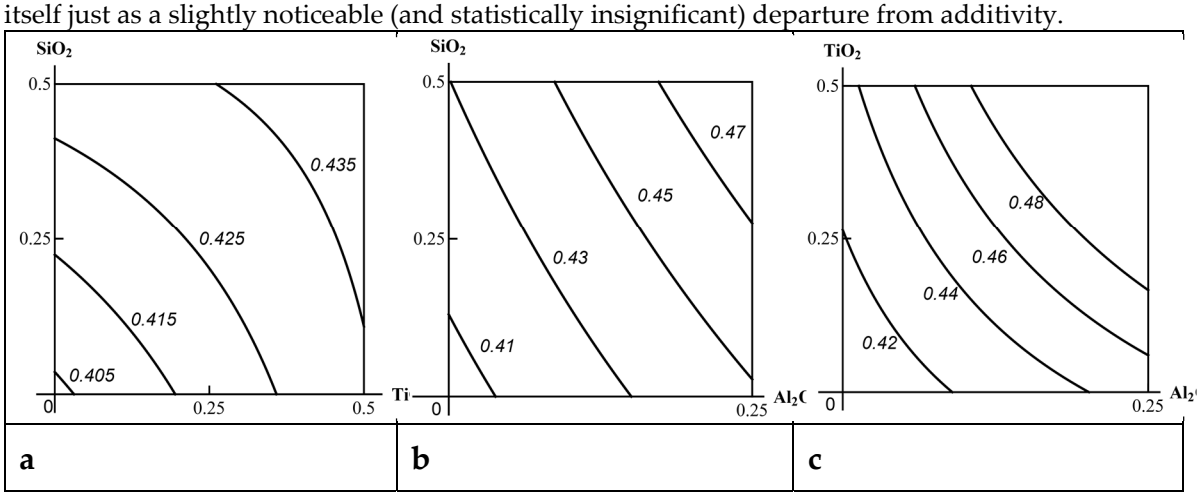

Preprints (www.preprints.org) | NOT PEER-REVIEWED | Posted: 25 January 2018 doi:10.20944/preprints201801.0238.v1

Peer-reviewed version available at Int. J. Mol. Sci. 2018, 19, 837; doi:10.3390/ijms19030837

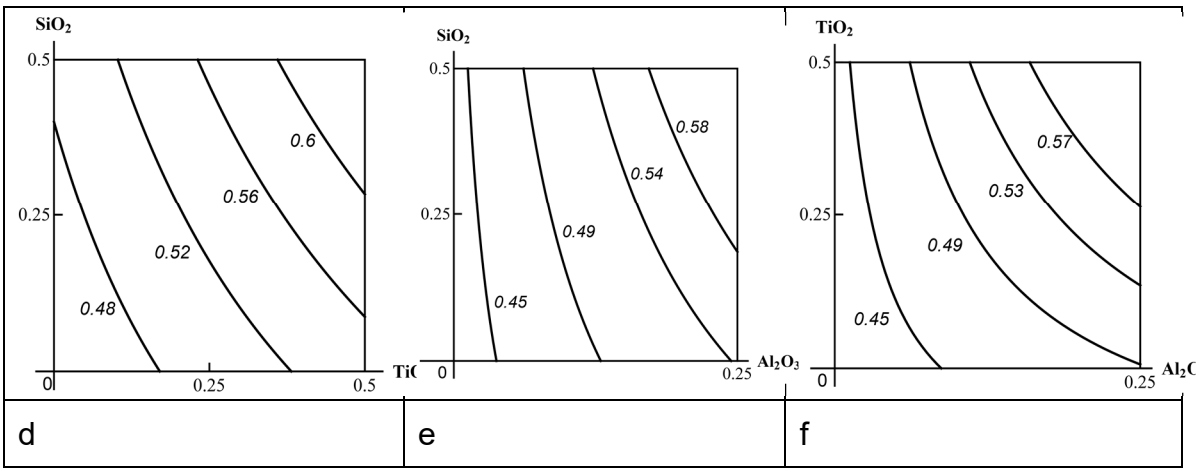

Figure 14. Isoboles of binary combined genotoxicity assessed by an increase in nucleated blood cell DNA fragmentation coefficient. **(A)** in the absence of a third factor under exposure to: (a) SiO_2-NP + TiO_2-NP (subadditivity); (b) SiO_2-NP + Al_2O_3-NP (additivity); (c) TiO_2-NP + Al_2O_3-NP (superadditivity). **(B)** with background administration of a third component: (d) Al_2O_3-NP к SiO_2-NP + TiO_2-NP (additivity); (e) TiO_2-NP к SiO_2-NP + Al_2O_3-NP (single-factor action with transformation into additivity); (f) SiO_2-NP to TiO_2-NP + Al_2O_3-NP (superadditivity). The axes represent corresponding MeO-NPs in mg per rat; the numbers at the isobole denote the dimensionless quantity Cfr.

In the context of the above classification of three-factor combined toxicity, comparison of isoboles for this or that binary combination in the absence or presence of a third factor provides evidence of the following. Where Al_2O_3-NP is considered as such a background factor, the explicit subadditivity of the actions of the other two components transforms into an additivity with a tendency towards superadditivity, i.e. into a type of combined action which is more adverse for the organism (class A). If the third factor is TiO_2-NP, the genotoxicity of the combination (SiO_2-NP + Al_2O_3-NP), being strictly additive without this factor, approaches a single-factor one determined mainly by the dose of Al_2O_3-NP, which is less adverse (class B). Finally, the addition of SiO_2-NP to the combination (TiO_2-NP + Al_2O_3-NP) did not actually change the superadditive type of its action (class C). Previously we had not come across such uncertainty of classification of three-factor toxicity for one and the same effect depending on which of these factors is considered as the third one. Bearing in mind the precaution principle, we believe it right to assess this ternary combination as pertaining to the most adverse class A, all the more so that this class was determined by the action of the factor (Al_2O_3-NP) that both alone and as a component of the binary combinations proved to be the most hazardous.

2.5. Efficacy of the Bioprotective Complex

Going back to the data presented in Table 3, note that the statistically significant protective effect of the BPC was revealed by the shifts caused by the ternary NP-combination in just a few indices (urea, reduced glutathione and ALT activity in blood serum: trombocyte and reticulcyte counts). At the same time, the same exposure with background administration of the BPC was accompanied by a statistically significantly enhanced leukocytosis, which, however, may be regarded as accidental because the action of the BPC by itself did not provoke this effect. BPC administration without exposure to the NPs gave a significant increase in body mass compared with the controls. Therefore the respective difference between the groups of ternary exposure without BPC and with BPC — being of the same sign although statistically insignificant — stands out as possibly beneficial, and all the more so that in the second case the body mass gain was higher than in the other groups which were not given the BPC, including the control one. The probability of such 5-fold coincidence being accidental is equal to 0.03 only.

Preprints (www.preprints.org) | NOT PEER-REVIEWED | Posted: 25 January 2018 doi:10.20944/preprints201801.0238.v1

Peer-reviewed version available at Int. J. Mol. Sci. 2018, 19, 837; doi:10.3390/ijms19030837

A much more explicit protective efficacy of the BPC was shown by the morphometrically assessed indices of toxic damage to the internal organs, which in Figure 15 is exemplified by damage to kidneys.

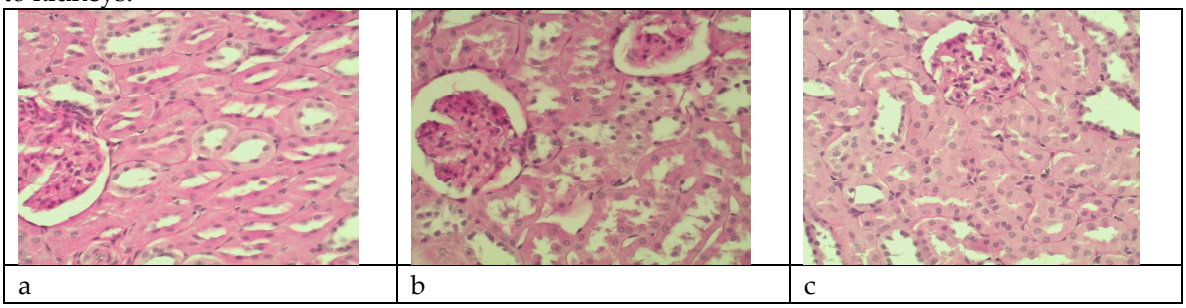

a b c

Figure 15. (a) Kidney of a control rat (proximal convoluted tubules with an intact brush border). (b) Kidney of a rat exposed to the ternary MeO-NP combination (marked degenerative and necrobiotic changes in tubular epithelial cells up to their disappearance; partial destruction of the brush border). (c) Kidney of a rat exposed to the same combination against background administration of the BPC. Periodic Acid Shiff (PAS) stain, magnification *400.

As follows from Table 5, in this case the brush border loss index was equal for the three-factor intoxication to 7.19 ± 1.47, whereas for the same intoxication with background BPC administration to just 1.99 ± 0.43 ($P<0.05$), only the former quantity being different from the control value (1.49 ± 0.56) statistically significantly. Inter-group differences of the same sign and statistical significance can be seen for epithelial desquamation as well.

Table 7 demonstrates the protective effect of the BPC in all three morphometric indices of hepatotoxicity of the full ternary MeO-NP combination, although it is statistically significant for one of them only (the most important one though), and in general is less pronounced than for the nephrotoxicity indices.

We believe that the most striking results were obtained by RAPD testing (Subsection 2.4.), which provide evidence of a rather high anti-genotoxic efficacy of the bioprotective complex tested. Indeed, as can been seen from Table 12, DNA fragmentation caused by exposure to nanoparticle combinations with the BPC being administered was attenuated even to greater degree than by halving the dose of the three MeO-NPs. Meanwhile, attaining a twofold reduction in any harmful occupational exposure under actual industrial conditions presents a rather expensive and challenging task.

3. Experimental Section

The experiment was carried out on outbred white male rats from our own breeding colony with the initial body weight of ca. 300 g,, with a minimum of 12 animals in each of the exposed and control groups. The rats were housed in conventional conditions, breathed unfiltered air, and were fed standard balanced food. The experiments were planned and implemented in accordance with the "International guiding principles for biomedical research involving animals" developed by the Council for International Organizations of Medical Sciences (1985) and were approved by the Ethics Committee of the Ekaterinburg Medical Research Center for Prophylaxis and Health Protection in Industrial Workers.

For this experiment, we prepared suspensions of metal oxide nanoparticles (MeO-NP) by laser ablation of 99.9% pure metal (Al and Ti) or semiconductor (Si) targets in sterile de-ionized water. The ablation was performed using an Fmark-20RL laser material processing system (Laser Technology Center, St. Petersburg, Russia) based on an ytterbium-doped pulsed fiber laser (pulse length 100 ns, repetition rate 21 kHz, wavelength 1064 nm). The energy density was about 80 J/cm^2. The targets were irradiated in scanning mode with the rate of the laser spot at 270 mm/s. At the beginning, seven scanning cycles were used for preparation of the target surface.

Preprints (www.preprints.org) | NOT PEER-REVIEWED | Posted: 25 January 2018 doi:10.20944/preprints201801.0238.v1

Peer-reviewed version available at Int. J. Mol. Sci. 2018, 19, 837; doi:10.3390/ijms19030837

A scanning electron microscope (SEM), CrossBeam Workstation Auriga (Carl Zeiss, Jena, Germany), was used for the visualization of the nanoparticles MPs. A Raman confocal microscope, Alpha 300 AR (WiTec, Ulm, Germany), was used for the analysis of the NP composition, found to be containing Al_2O_3, TiO_2 and SiO_2, respectively.

The concentration of the TiO_2-NP and SiO_2-NP suspensions was increased to 0.5 mg/mL by partial evaporation of the primary suspensions for 5 h at 50 °C. We were unable to concentrate the Al_2O_3-NP suspension without destabilization to any level greater than 0.25 mg/mL.

The nanoparticles in all the suspensions were of spherical shape (as an example, the SEM image of the Al_2O_3-NP is shown in Figure 16). The average particle diameter (±s.d.) obtained by statistical processing of hundreds of scanning electron microscopy (SEM) images was 21±6 nm for Al_2O_3-NP, 27±7 nm for TiO_2-NP and 43±11 for SiO_2-NP. The distribution functions (Figure 17) were symmetrical in all three cases.

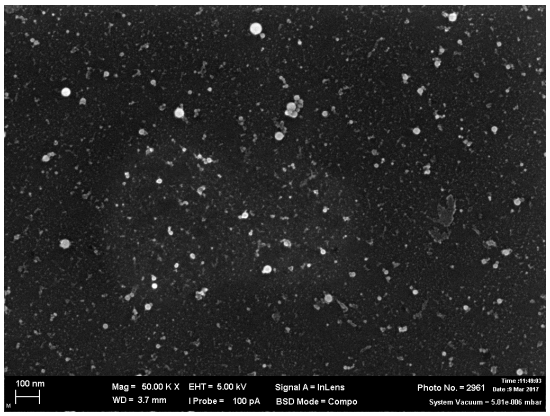

Figure 16. SEM images of Al_2O_3 nanoparticles in the suspension obtained by scanning electron microscopy with magnification *50,000.

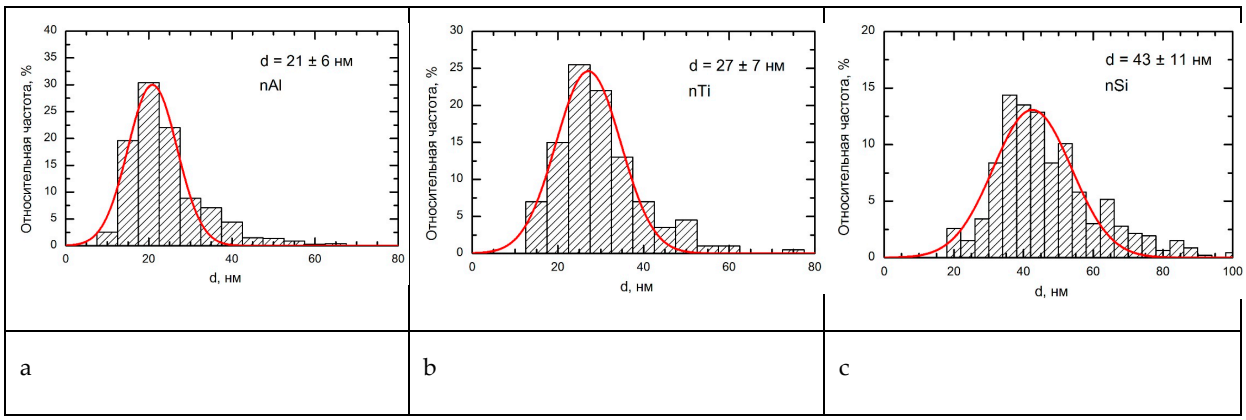

Figure 17. Size distribution function obtained by statistical processing of SEM images of Al_2O_3-NP (a), TiO_2-NP (b) and SiO_2-NP (c).

The absence of noticeable changes in the zeta potential as well as in the shape and position of the plasmon resonance peak 30 days after suspension preparation confirmed the high stability of all the NiO-NPs suspensions.

As well as in our previous nano-toxicological experiments, for modeling subchronic intoxication with metal-oxide nanoparticles (MeO-NP), each nanomaterial was administered to a rat by intraperitoneal (IP) injections three times a week (up to 18 injections) at a dose of 0.5 mg of TiO_2-NP and SiO_2-NP or 0.25 mg of Al_2O_3-NP per rat (i.e., about 2.5 and 1.25 mg/kg body mass, respectively) in 1 mL of the suspension. To avoid direct interactions between chemically different NPs resulting in their fast aggregation, different NP suspensions were drawn into different syringes and injected

Preprints (www.preprints.org) | NOT PEER-REVIEWED | Posted: 25 January 2018 doi:10.20944/preprints201801.0238.v1

Peer-reviewed version available at Int. J. Mol. Sci. 2018, 19, 837; doi:10.3390/ijms19030837

separately to the rats of the combined exposure group, one after another, at an interval of about 1 min.

The groups of rats being investigated in parallel were administered either one MeO-NP species alone in the above-mentioned doses plus 2 mL of deionized water; or one of the three possible binary combinations of these MeO-NPs (Al_2O_3-NP + TiO_2-NP; Al_2O_3-NP + TiO_2-NP; SiO_2-NP+TiO_2-NP) plus 1 mL of deionized water; or a ternary combination of the same MeO-NP in the same doses; or the same ternary combination at half dose (This group was included into the design of the experiment mainly in order to increase the stability of the response surface and thereby the reliability of this mathematical model of combined action (see below). At the same time, as was shown in Section 2, comparison of the indices in this group and in the full-dose one pointed to the presence of a dose-effect dependence, which is an important toxicological argument in favor of the causal relationship); or 3 mL of deionized water without any NPs. Thus, the total volume of intraperitoneally injected liquid was equal to 3 mL in all groups. Half of the rats in the latter two of the above groups received throughout the exposure period a bioprotective complex (BPC), including:

(1) Glutamate as an effective cell membrane stabilizer acting through the intensification of ATP synthesis under exposure to the damaging effect of various cytotoxic particles and, at the same time, as one of the precursors of glutathione, which is a powerful cell protector against oxidative stress as, presumably, one of the key mechanisms underlying the cytotoxicity and genotoxicity of virtually all metallic NPs.

(2) The other two glutathione precursors: glycine and cysteine (the latter in a highly active and metabolically well available form of N-acetylcysteine).

(3) Other agents of the organism's anti-oxidant system (vitamins A, E, and C, and selenium).

(4) Omega-3 polyunsaturated fatty acids whose intracellular derivatives — eicosanoids — activate DNA replication and thus play an important part in its repair.

(5) Iodine, taking into consideration the well-known disturbances of the thyroid function caused by some metallic intoxications.

(6) Essential elements known to be antagonists of the metal that forms Me-NPs under study.

(7) Pectin enterosorbent as an agent that hinders the re-absorption of toxic metals excreted into the intestines with bile.

The doses and administration methods of these bio-protectors are given in Table 13

Table 13. Doses and Mode of Administration of the Bioprotectors Tested in Our Experiment.

Bioprotectors	Estimated Dosage and Mode of Administration
Apple pectin	1 g/kg (added to the fodder)
Sodium glutamate	160 mg per rat (as a 1.5% drink instead of water)
Glycine	12 mg per rat (added to the food)
N-Acetylcysteine	30 mg per rat (added to the food)
Vitamin C	4.4 mg per rat (added to the food)
Vitamin E	0.84 mg per rat (added to the food)
Selenium	4.0 mcg per rat (added to the food)
Commercial fish oil rich in vitamin A and omega 3 PUFA	1 drop per rat (sublingually)
Potassium iodide	4.0 mcg per rat (added to the food)
Calcium carbonate	160 mg per rat (added to the food)

We gave glutamate to the rats as 1.5% solution instead of drinking water *ad libitum*. The "Amber Dew" (Ecco-Plus Ltd.: Zhukovskiy, Russia), a fish oil preparation rich in PUFA mainly of the ω-3 group (24%), was administered through gavage at a dose of 1 mL per rat. Apple pectin enterosorbent (Promavtomatika Ltd.: Belgorod, Russia) was added to the rats' food in a quantity corresponding to a dose of ca. 1000 mg/kg body weight. Commercial preparations of iodide, amino acids and vitamins available as tablets were crushed and added to another portion of the food in quantities

Preprints (www.preprints.org) | NOT PEER-REVIEWED | Posted: 25 January 2018 doi:10.20944/preprints201801.0238.v1

Peer-reviewed version available at Int. J. Mol. Sci. 2018, 19, 837; doi:10.3390/ijms19030837

corresponding to recommended daily intake of these micronutrients for rats (where such recommendations were known only for humans, a recalculation to the rats nutritional requirements was made based on the species standard metabolism ratio).

Taking into consideration that the standard balanced food presumably meets the normal nutritional requirements of a rat, we assumed that additional intake of the above-listed bioactive substances would meet the increased needs connected with the molecular mechanisms of metallic NP toxicity. Nevertheless, it had to be checked whether or not such presumed overloading with them would evoke any unfavorable effects. That is why in our experiment one group of rats was administered the same BPC but was not exposed to any toxicant.

Immediately after the end of the exposure period, the following procedures were performed for all rats:

- Weighing of body.
- Estimation of the CNS ability to evoke temporal summation of sub-threshold impulses (a variant of the withdrawal reflex and its facilitation by repeated electrical stimulations in an intact, conscious rat).
- Recording of the number of head-dips into the holes of a hole-board (which is a simple but informative index of exploratory activity frequently used for studying the behavioral effects of toxicants and drugs).
- Collection of daily urine for analysis of its output (diuresis), specific gravity (density), protein, total coproporphyrin, δ-aminolevulinic acid (δ-ALA), urea, uric acid, creatinine.

Then the rats were killed by quick decapitation and blood was collected by exsanguination. The liver, spleen, kidneys, and brain were weighed. The biochemical indices determined from the blood included reduced glutathione (GSH), total serum protein, albumin, globulin, bilirubin, ceruloplasmin, malonyl dialdehyde (MDA), alkaline phosphatase, alanine- and aspartate-transaminases (ALT, AST), catalase, gamma glutamyl transferase, SH-groups, urea, uric acid, creatinine, thyrotropic hormone of hypophysis, thyroxin, and triiodothyronine. For determining hemoglobin content, hematocrit, mean erythrocyte volume and for counting RBC, WBS and thrombocytes, we used the MYTHIC-18 auto-hematology analyzer. Reticulocyte percentage was counted using the routine technique. Cytochemical determination of succinate dehydrogenase (SDH) activity in lymphocytes was based on the reduction of nitrotetrazolium violet to formazan, the number of granules of which in a cell was counted under immersion microscopy.

All the clinical laboratory tests on blood and urine with the exception of specially stipulated ones were performed using well-known techniques described in many manuals.

Liver, spleen, kidney, and brain tissue sections were prepared from four rats from each treated and control group for histological examination by the hematoxilin and eosin stain and, when necessary, PAS, Nissl or Perl's stain. For morphometric characterization of these tissues, we used the Avtandilov's planimetric ocular grid and the image recognition programmed system CellSens (Olympus, Hamburg, Germany).

Also, tissue touching imprints were made from the surfaces of freshly cut liver, kidneys, spleen and mesenteric lymph nodes on a glass slide, which were dried at room temperature and stained by Leishman's stain. The cell composition and signs of cell damage were estimated under a binocular light microscope, Carl Zeiss Primo Star with a USCMOS imaging camera at 100x and 1000x. Microscopy involved counting 100 cells from each lymph node imprint and 300 cells from the imprints of other organs.

The *in vivo* subchronic genotoxic effect was estimated with the Random Amplification of Polymorphic DNA (RAPD) test on blood nucleated cells. The samples were collected into special vessels cooled to −80 °C. These were then promptly delivered in cryo-containers to a specialized laboratory. To isolate DNA from the cells, we used a GenElute (Sigma, St. Louis, MO, USA) set of reagents in accordance with the manufacturer's guidelines for use. The DNA content of the samples was determined spectrophotometrically (Ultraspec 1100 pro; Amersham Biosciences Ltd.: Amersham, UK); these were then frozen and stored at −84 °C in a kelvinator (Sanyo Electric Co., Ltd.: Moriguchi, Japan) till the beginning of the RAPD test. The method is based on the fact that, unlike a

Preprints (www.preprints.org) | NOT PEER-REVIEWED | Posted: 25 January 2018 doi:10.20944/preprints201801.0238.v1

Peer-reviewed version available at Int. J. Mol. Sci. 2018, 19, 837; doi:10.3390/ijms19030837

fragmented DNA, which, in the agarose gel electrophoresis, forms the so-called comet tail, a non-fragmented DNA has a very low degree of migration and stays virtually in the same place (comet head), the degree of migration being directly related to the degree of DNA fragmentation. DNA amplification was carried out using specific primers and tritiated nucleotides. To characterize the degree of damage to DNA we used the "coefficient of fragmentation", i.e., the ratio of total radioactivity of all tail fractions to that of the head. Each blood sample was analyzed in three replications.

For all toxicity indices measured in this experiment, the statistical significance of the differences between the group arithmetic mean values was estimated using Student's *t* test with Bonferroni correction for multiple comparisons, but the tables of results presented in this paper do not specify it for the groups, comparing which would be pointless.

Mathematical modeling of responses to binary exposures was based on the Response Surface Method (RSM) [57, 58]. In this methodology, equation (1) describing the response surface $Y = Y(x_1, x_2)$ can be constructed by fitting its coefficients to experimental data.

$$Y = f\left(x_1, x_2\right) \qquad (1)$$

where Y is the quantitative effect (outcome) of a toxic exposure; x_1 and x_2 are the doses of the toxicants participating in the combination; $f(x_1, x_2)$ is a regression equation with some numeric parameters. In the case of two-level exposures (even if one of the levels is equal to zero), the response surface may have one possible shape (hyperbolic paraboloid)

$$Y = b_0 + b_1x_1 + b_2x_2 + b_{12}x_1x_2 \qquad (2)$$

It is inferred that two agents produce a unidirectional effect on response Y if both one-way response functions $Y(x_1, 0)$ and $Y(0, x_2)$ either increase or decrease with an increase in x_1 or x_2; on the contrary, two agents are assumed to be acting contra-directionally (oppositely) if one function increases while the other decreases. This mathematical model enables one to predict the magnitude of response Y for any combination of toxicant doses within the experimental range for each of them (rather than at two factual points only). The sectioning of the response surface on different levels corresponding to different meanings of the outcome **Y** or of the doses **x,** provides a family of Loewe isoboles that may have the same or a different form and/or different slopes and thus render the interpretation of binary combined toxicity types both easy and illustrative. In Section 2, we therefore discussed the results of the RSM modeling presented just in this way.

For risk-oriented mathematical description of three-factorial toxicity, we took advantage of the original approach that we had proposed and used previously [16, 59].

Conclusions

Compared with the nanoparticles of manganese, nickel, lead, zinc and – twice – copper oxides previously tested by us in experiments of similar design, the subchronic intoxication that developed under the impact of the MeO-NPs investigated in this study was characterized by a relatively small number of functional and biochemical indices of the changed organism's integral status, with no signs specific to the toxicodynamics of this or that toxic agent revealed. At the same time, the morphometric indices (in full agreement with what we had observed previously) and cytological indices of toxic damage to the kidneys, liver and spleen (measured for the first time in our studies) provided evidence of the undoubted organ toxicity of all the MeO-NP species studied, with this toxicity found to be qualitatively of similar type for different NP species but pronounced to a different degree. Also in full agreement with the previously gained data, the RAPD test revealed that the nano-intoxications studied involved enhanced genomic DNA fragmentation. For the majority of these adverse effects, aluminum oxide nanoparticles proved to be the most noxious.

As for the typology of combined toxicity, our new results are also essentially in agreement with the previously obtained data not only for other MeO-NPs but also for metal ions, confirming that this typology may be ambiguous for one and the same pair of toxic agents depending on the dose ratio, on specific effect for which this toxicity is assessed and, often, on the level of this effect.

Preprints (www.preprints.org) | NOT PEER-REVIEWED | Posted: 25 January 2018 doi:10.20944/preprints201801.0238.v1

Peer-reviewed version available at Int. J. Mol. Sci. 2018, 19, 837; doi:10.3390/ijms19030837

Methodologically, a new confirmation has been obtained for the Response Surface Method as an adequate tool for mathematical modeling of combined toxicity.

The fact that one of the components in a ternary Me-NP combination operating in the background may modify the type of combined toxicity displayed by the other two towards either a higher or lower risk or remain essentially unchanged was established by us for the first time as a common pattern of three-factorial toxicity of metals in ion-molecular form [16] and later on, in experiments with CuO, PbO-NP and ZnO nanoparticles [59] and again in the present study. Even though the most adverse variant of three-factorial toxicity was shown only for a proportion of outcomes, we maintain that the precautionary principle should orient our attention just to this variant when analyzing multi-factorial occupational health risks. At the same time, we have proved once more that even additionally enhanced effects of a ternary nano-combination (including the additive or even superadditive genotoxicity) could be substantially attenuated with a complex of bioprotectors acting beneficially through various mechanisms.

There is no doubt that in the light of the challenges of assessing and managing occupational health risks in a specific industry all the obtained results are of *practical value* inasmuch as they are new for the *given* combination of toxics irrespective of the fact that they may be similar to those obtained for other combinations. At the same time, for the development of the *general theory* of combined nano-toxicity, it is just this fundamental repeatability of the most important inferences from different studies of our team, several times highlighted in this paper, that we believe to be the most interesting and important finding.

References

1. Katsnelson, B.A; Privalova, L.I; Degtyareva, T.D; Sutunkova, M.P., Yeremenko, O.S., Minigalieva, I.A. Experimental estimates of the toxicity of iron oxide Fe_3O_4 (magnetite) nanoparticles. Cent Eur J Occup Environ Med. **2010**, 16, 47–63.
2. Katsnelson, B.A; Privalova, L.I; Kuzmin, S.V; Degtyareva, T.D., Sutunkova, M.P., Yeremenko, O.S. Some peculiarities of pulmonary clearance mechanisms in rats after intratracheal instillation of magnetite (Fe_3O_4) suspensions with different particle sizes in the nanometer and micrometer ranges: Are we defenseless against nanoparticles? Int J Occup Environ Health. **2010**, 16, 508–524. doi:10.1179/107735210799160011
3. Katsnelson, B.A; Degtyareva, T.D; Minigalieva, I.A; Privalova, L.I.; Kuzmin, S.V.; Yeremenko, O.S.; Kireyeva, E.P.; Sutunkova, M.P.; Valamina I.I.; Khodos, M.Y.; Kozitsina, A.N.; Shur, V.Y.; Vazhenin, V.A.; Potapov, A.P.; Morozova, M.V. Sub-chronic systemic toxicity and bio-accumulation of Fe_3O_4 nano- and microparticles following repeated intraperitoneal administration to rats. Int J Toxicol. **2011**, 30, 60–67. doi:10.1177/1091581810385149
4. Katsnelson, B.A; Privalova, L.I; Kuzmin, S.V; Gurvich, V.B.; Sutunkova, M.P.; Kireyeva, E.P.; Minigalieva I.A. An approach to tentative reference levels setting for nanoparticles in the workroom air based on comparing their toxicity with that of their micrometric counterparts: A case study of iron oxide Fe3O4. J ISRN Nanotechnol. **2012**, 2012, 12. doi:10.5402/2012/143613
5. Katsnelson, B.A.; Privalova, L.I.; Sutunkova, M.P.; Khodos, M.Y.; Shur, V.Y.; Shishkina, E.V.; Tulakina, L.G.; Pichugova, S.V.; Beikin J.B. Uptake of some metallic nanoparticles by, and their impact on pulmonary macrophages *in vivo* as viewed by optical, atomic force, and transmission electron microscopy. J Nanomed Nanotechnol. **2012**, 3, 1–8.
6. Katsnelson, B.A.; Privalova, L.I.; Sutunkova, M.P.; Tulakina, L.G.; Pichugova, S.V.; Beikin, J.B.; Khodos M.J. The *"in vivo"* interaction between iron oxide Fe_3O_4 nanoparticles and alveolar macrophages. J Bull Exp Biol Med. **2012**, 152, 627–631.
7. Katsnelson, B.A.; Privalova, L.I.; Gurvich, V.B.; Makeyev, O. H.; Shur, V. Ya.; Beikin, Y. B.; Sutunkova, M. P.; Kireyeva, E. P.; Minigalieva, I. A.; Loginova, N. V.; Vasilyeva, M. S.; Korotkov, A. V.; Shuman, E. A.; Vlasova, L. A.; Shishkina, E. V.; Tyurnina, A. E.; Kozin, R. V.; Valamina, I. E.; Pichugova, S. V.; Tulakina L. G. Comparative *in vivo* assessment of some adverse bio-effects of equidimensional gold and silver nanoparticles and the attenuation of nanosilver's effects with a complex of innocuous bioprotectors. Int J Mol Sci. **2013**, 14, 2449–2483. doi:10.3390/ijms14022449

Preprints (www.preprints.org) | NOT PEER-REVIEWED | Posted: 25 January 2018 doi:10.20944/preprints201801.0238.v1

Peer-reviewed version available at Int. J. Mol. Sci. 2018, 19, 837; doi:10.3390/ijms19030837

8. Katsnelson, B.A.; Minigalieva, I.A.; Privalova, L.I.; Sutunkova, M.P.; Gurvich, V.B.; Shur, V. Ya.; Shishkina, E.V.; Varaksin, A.N.; Panov, V.G. Lower airways response in rats to a single or combined intratracheal instillation of manganese and nickel nanoparticles and its attenuation with a bio-protective pre-treatment. J Toksicol Vestnik. **2014**, 6, 8–14.
9. Privalova, L.I.; Katsnelson, B.A.; Loginova, N.V.; Gurvich, V.B.; Shur, Ya.V.; Beikin, Y.B.; Sutunkova, M.P.; Minigalieva, I.A.; Shishkina, E.V.; Pichugova, S.V.; Tulakina, L.G.; Beljaeva, S.V. Some Characteristics of Free Cell Population in the Airways of Rats after Intratracheal Instillation of Copper-Containing Nano-Scale Particles. Int J Mol Sci. **2014**, 15, 21538–21553. doi:10.3390/ijms151121538
10. Privalova, L.I.; Katsnelson, B.A.; Loginova, N.V.; Gurvich, V.B.; Shur, V.Y.; Valamina, I.E.; Makeyev, O.H.; Sutunkova, M.P.; Minigalieva, I.A.; Kireyeva, E.P.; Rusakov, V.O.; Tyurnina, A.E.; Kozin, R.V.; Meshtcheryakova, E.Y.; Korotkov, A.V.; Shuman, E.A.; Zvereva, A.E.; Kostykova S.V. Subchronic Toxicity of Copper Oxide Nanoparticles and Its Attenuation with the Help of a Combination of Bioprotectors. Int J Mol Sci. **2014**, 15, 12379–12406. doi:10.3390/ijms150712379
11. Minigalieva, I.A.; Katsnelson, B.A.; Privalova, L.I.; Sutunkova, M.P.; Gurvich, V.B.; Shur, V.Y.; Shishkina, E.V.; Valamina, I.E.; Makeyev, O.H.; Panov, V.G.; Varaksin, A.N.; Grigoryeva, E.V.; Meshtcheryakova E.Y. Attenuation of combined nickel (II) oxide and manganese (II,III) oxide nanoparticles' adverse effects with a complex of bioprotectors. Int J of Mol Sci. **2015**, 16(9), 22555-22583. doi:10.3390/ijms160922555
12. Katsnelson, B.A.; Minigaliyeva, I.A.; Panov, V.G.; Privalova. L.I.; Varaksin, A.N.; Gurvich, V.B.; Sutunkova. M.P.; Shur, V.Ya.; Shishkina, E.V.; Valamina, I.E.; Makeyev, O.H. Some patterns of metallic nanoparticles' combined subchronic toxicity as exemplified by a combination of nickel and manganese oxide nanoparticles. J Food Chem Toxicol. **2015**, 86, 351-364. doi:10.1016/j.fct.2015.11.012
13. Katsnelson, B.A.; Privalova, L.I.; Sutunkova, M.P.; Minigalieva, I.A.; Gurvich, V.B.; Shur, V.Y.; Makeyev, O.H.; Valamina, I.E.; Grigoryeva, E.V. Is it possible to enhance the organism's resistance to toxic effects of metallic nanoparticles? J Toxicol. **2015**, 337, 79-82. doi:10.1016/j.tox.2015.09.001
14. Katsnelson, B.A.; Privalova, L.I.; Sutunkova, M.P.; Gurvich, V.B.; Minigalieva, I.A.; Loginova, N.V.; Kireyeva, E.P.; Shur, V.Ya.; Shishkina, E.V.; Beikin, Ya. B.; Makeyev, O.H.; Valamina I.E. Some inferences from in vivo experiments with metal and metal oxide nanoparticles: the pulmonary phagocytosis response subchronic systemic toxicity and genotoxicity, regulatory proposals, searching for bioprotectors (a self-overview). Int. J. Nanomed. **2015**, 10, 3013–3029.
15. Sutunkova, M.P.; Katsnelson, B.A.; Privalova, L.I.; Gurvich, V.B.; Konysheva, L.K.; Shur, V.Ya.; Shishkina, E.V.; Minigalieva, I.A.; Solovjeva, S.N.; Grebenkina, S.V.; Zubarev, I.V. On the contribution of the phagocytosis and the solubilization to the iron oxide nanoparticles retention in and elimination from lungs under long-term inhalation exposure. J Toxicol, **2016**, 363, 19-28. doi:10.1016/j.tox.2016.07.006
16. Minigalieva, I.A.; Katsnelson, B.A.; Panov, V.G.; Privalova, L.I.; Varaksin A.N.; Gurvich, V.B.; Sutunkova M.P.; Shur V.Ya.; Ekaterina V. Shishkina, Irene E. Valamina, Ilya V. Zubarev, Oleg H. Makeyev, Ekaterina Y. Meshtcheryakova, Svetlana V. KlinovaIn vivo toxicity of copper oxide, lead oxide and zinc oxide nanoparticles acting in different combinations and its attenuation with a complex of innocuous bio-protectors. Toxicology. **2017**, 380, 72-93.
17. Katsnelson, B.A.; Privalova L.I.; Sutunkova, M.P.; Minigalieva, I.A.; Gurvich V.B.; Shur V.Y.; Shishkina E.V.; Makeyev, O.H.; Valamina I.E.; Varaksin A.N; Panov V.G. Experimental research into metallic and metal oxide nanoparticle toxicity *in vivo*, In: B. Yan, H. Zhou, J. Gardea-Torresdey (Eds.). "Bioactivity of Engineered Nanoparticles", Springer, **2017**, Chapter 11., 259-319.
18. Minigalieva, I.A.; Bushueva, T.V., Froehlich E. Are in vivo and in vitro assessments of comparative and combined toxicity of the same metallic nanoparticles compatible, or contradictory, or both? A juxtaposition of data obtained in respective experiments with NiO and Mn3O4 nanoparticles. Food and Chmic Toxicol. **2017**, 109, 393-404.
19. Vance, M.E., Kuiken, T., Vejerano, E.P.; McGinnis S.P.; Hochella Jr M.F.; Rejeski D.; Hull M.S. Nanotechnology in the real world: redeveloping the nanomaterials consumer products inventory. Beilstein J. Nanotechnol. **2015**, 6, 1769–1780.
20. Bermudez, E.; Mangum, J.B; Wong, B.A; Asgharian B.; Hext P.M.; Warheit D.B.; Everitt J.I Pulmonary responses of mice, rats, and hamsters to subchronic inhalation of ultrafine titanium dioxide particles. Toxicol Sci. **2004**, 77(2), 347-57.

Preprints (www.preprints.org) | NOT PEER-REVIEWED | Posted: 25 January 2018 doi:10.20944/preprints201801.0238.v1

Peer-reviewed version available at Int. J. Mol. Sci. 2018, 19, 837; doi:10.3390/ijms19030837

21. Grassian, V.H.; O'Shaughnessy, P.T.; Adamcakova-Dodd A.; Pettibone J.M.; Thorne P.S. Inhalation exposure study of titanium dioxide nanoparticles with a primary particle size of 2 to 5 nm. Environ. Health Perspect. **2007**, 115, 397–402.
22. Warheit, D.B; Webb, T.R; Reed, K.L; Frerichs, S.; Sayes, C.M. Pulmonary toxicity study in rats with three forms of ultrafine-TiO2 particles: differential responses related to surface properties. Toxicology. **2007**, 230, 90–104.
23. Geiser, M; Casaulta, M; Kupferschmid, B; Schulz, H.; Semmler-Behnke, M.; Kreyling, W. The role ofmacrophages in the clearance of inhaled ultrafine titaniumdioxide particles. Am. J. Respir. Cell Mol. Biol. **2008**, 38, 371–376.
24. Liu, R.; Yin, L.; Pu, Y.; Liang, G.; Zhang, J.; Su, Y.; Xiao, Z.; Ye, B. Pulmonary toxicity induced by three forms of titanium dioxide nanoparticles via intra-tracheal instillation in rats. Prog. Nat. Sci. **2009**, 19, 573–579.
25. Park, E.-J.; Yoon, J; Choi, K; Yi, J.; Park K. Induction of chronic inflammation in mice treated with titanium dioxide nanoparticles by intratracheal instillation. Toxicology. **2009**, 260, 37–46.
26. Iavicoli, I.; Leso, V.; Fontana, L.; Bergamaschi, A. Toxicological effects of titanium dioxide nanoparticles: a review of in vitro mammalian studies. Eur. Rev. Med.Pharmacol. Sci. **2011**, 15, 481–508.
27. Husain, M; Saber, A.T; Guo, C, Jacobsen, N.R; Jensen, K.A.; Yauk, C.L.; Williams, A.; Vogel, U.; Wallin, H.; Halappanavar, S. Pulmonary instillation of low doses of titanium dioxide nanoparticles in mice leads to particle retention and gene expression changes in the absence of inflammation. Toxicology and Applied Pharmacology. **2013**, 269, 250–262.
28. Shakeel, M; Jabeen, F; Iqbal R.; Chaudhry A.S.; Zafar, S.; Ali, M.; Khan, M.S.; Khalid, A.; Shabbir, S.; Asghar, M.S. Assessment of titanium dioxide nanoparticles (TiO2-NPs) Induced hepatotoxicity and ameliorative effects of Cinnamomum cassia in Sprague-Dawley rats/ Biological Trace Element Research. **2017**, 1-13 doi: 10.1007/s12011-017-1074-3
29. Hong, F; Zhou, Y; Zhao, X; Sheng, L.; Wang, L. Maternal exposure to nanosized titanium dioxide suppresses embryonic development in mice. Int J Nanomedicine. **2017**, 12, 6197-6204.
30. Kreyling, W.G; Holzwarth, U.; Haberl, N.; Kozempel, J.; Hirn, S.; Wenk, A.; Carsten, S.; Schäffler, M.; Lipka, J.; Semmler-Behnke, M.; Gibson, N. Quantitative Biokinetics of Titanium Dioxide Nanoparticles After Intravenous Injection in Rats: Part 1 Nanotoxicology. **2017**, 11 (4), 434-442.
31. Kreyling, W.G; Holzwarth, U.; Haberl, N.; Kozempel, J.; Hirn, S.; Wenk, A.; Carsten, S.; Schäffler, M.; Lipka, J.; Semmler-Behnke, M.; Gibson, N. Quantitative Biokinetics of Titanium Dioxide Nanoparticles After Oral Application in Rats: Part 2 Nanotoxicology. **2017**, 11 (4), 443-453.
32. Kreyling, W.G; Holzwarth, U.; Haberl, N.; Kozempel, J.; Hirn, S.; Wenk, A.; Carsten, S.; Schäffler, M.; Lipka, J.; Semmler-Behnke, M.; Gibson, N.Quantitative Biokinetics of Titanium Dioxide Nanoparticles After Intratracheal Instillation in Rats: Part 3 Nanotoxicology. **2017**, 11 (4), 454-464.
33. Park, E.J; Park, K. Oxidative stress and pro-inflammatory responses induced by silica nanoparticles in vivo and in vitro. Toxicol. Lett. **2009**, 184 (1), 18–25.
34. Eom, H.J, Choi, J. Oxidative stress of silica nanoparticles in human bronchial epithelial cell, Beas-2B. Toxicol. In Vitro. **2009**, 23 (7), 1326–1332.
35. Kim, Y.J; Yu, M; Park, H.O; Yang, S.I. Comparative study of cytotoxicity, oxidative stress and genotoxicity induced by silica nanomaterials in human neuronal cell line. Mol. Cell. Toxicol. **2010**, 6 (4), 336–343.
36. Sergent, J.A; Paget, V; Chevillard, S. Toxicity and genotoxicity of nano-SiO_2 on human epithelial intestinal HT-29 cell line. Ann. Occup. Hyg. **2012**, 56 (5),622–630.
37. Tetsuka, E.; Shimizu, Y; Teruya, K.; Myojin-Maekawa, Y.; Shimamoto, F.; Watanabe, H.; Nakamichi, N. Liver injury induced by 30- and 50-nm-diameter silica nanoparticles. J-STAGE. **2012**, 36(3). http://doi.org/10.1248/bpb.b12-00738
38. Du, Z.J.; Zhao, D.L.; Jing, L.; Cui, G.; Jin, M.; Li, Y.; Liu, X.; Liu, Y.; Du, H.; Guo, C.; Zhou, X.; Sun, Z. Cardiovascular toxicity of different sizes amorphous silica nanoparticles in rats after intratracheal instillation. Cardiovasc. Toxicol. **2013**, 13 (3), 194–207.
39. Guo, C.; Xia, Y.; Niu, P; Jiang, L.; Duan, J.; Yu, Y.; Zhou, X.; Li, Y; Sun, Z. Silica nanoparticles induce oxidative stress, inflammation, and endothelial dysfunction in vitro via activation of the MAPK/Nrf2 pathway and nuclear factor-κB signaling. Int. J. Nanomed. **2015**, 10, 1463-1477

Preprints (www.preprints.org) | NOT PEER-REVIEWED | Posted: 25 January 2018 doi:10.20944/preprints201801.0238.v1

Peer-reviewed version available at Int. J. Mol. Sci. 2018, 19, 837; doi:10.3390/ijms19030837

40. Petrick, L.; Rosenblat, M.; Paland, N.; Aviram, M. Silicon dioxide nanoparticles increase macrophage atherogenicity: stimulation of cellular cytotoxicity, oxidative stress, and triglycerides accumulation. Environ. Toxicol. **2016**, 31 (6), 713–723.
41. Guo, C.; Yang, M.; Jing l. Amorphous silica nanoparticles trigger vascular endothelial cell injury through apoptosis and autophagy via reactive oxygen species-mediated MAPK/Bcl-2 and PI3K/Akt/mTOR signaling. Int. J. Nanomed. **2016**, 11:5257—5276.
42. Ren, L.; Zhang, J.; Zou, Y.; Zhang, L.; Wei, J.; Shi, Z.; Li, Y.; Guo, C.; Sun, Z.; Zhou, X. Silica nanoparticles induce reversible damage of spermatogenic cells via RIPK1 signal pathways in C57 mice. Int J Nanomedicine. **2016**, 11, 2251–2264. doi: 10.2147/IJN.S102268
43. Wang, J.; Yu, Y.; Lu, K. Silica nanoparticles induce autophagy dysfunction via lysosomal impairment and inhibition of autophagosome degradation in hepatocytes. Int. J. of Nanomed. 2017, 12, 809–825.
44. Murugadoss, S.; Lison, D.; Godderis, L.; Van Den Brule, S.; Mast, J.; Brassinne, F.; Sebaihi, N.; Hoet, P.H. Toxicology of silica nanoparticles: an update. Arch Toxicol. **2017**, 91(9), 2967-3010. doi: 10.1007/s00204-017-1993-y.
45. Orlando, A.; Cazzaniga, E.; Tringali, M.; Gullo, F.; Becchetti. A.; Minniti, S.; Taraballi, F.; Tasciotti, E.; Re, F. Mesoporous silica nanoparticles trigger mitophagy in endothelial cells and perturb neuronal network activity in a size- and time-dependent manner International Journal of Nanomedicine. **2017**, 12:3547–3559.
46. Chan, W.T.; Liu, C.C.; Chiang Chiau, J.S.; Tsai, S.T.; Liang, C.K.; Cheng, M.L.; Lee, H.C.; Yeung, C.Y.; Hou, S.Y. In vivo toxicologic study of larger silica nanoparticles in mice. International Journal of Nanomedicine. **2017**, 12, 3421–3432.
47. Sutunkova, M.P.; Solovyeva, S.N.; Katsnelson, B.A; Gurvich, V.B.; Privalova, L.I.; Minigalieva, I.A.; Slyshkina, T.V.; Valamina, I.E.; Makeyev, O.H.; Shur, V.Ya.; Zubarev, I.V.; Kuznetsov, D.K.; Shishkina, E.V. A paradoxical response of the rat organism to long-term inhalation of silica containing submicron (predominantly nanoscale) particles of a collected industrial aerosol at realistic exposure levels. Toxicology. **2017**, 384, 59-68.
48. Arul Prakash, F.; Dushendra Babu, G.J.; Lavanya, M., Shenbaga Vidhya, K.; Devasena T. Toxicity Studies of Aluminium Oxide Nanoparticles in Cell Lines. International Journal of Nanotechnology and Applications. **2011**, 5(2), 99-107 http://www.ripublication.com/ijna.htm
49. Radziun, E.; Dudkiewicz Wilczyńska, J.; Książek. Assessment of the cytotoxicity of aluminum oxide nanoparticles on selected mammalian cells. I Toxicol In Vitro.**2011**, 25(8), 1694-700. doi: 10.1016/j.tiv.2011.07.010.
50. Park, E.J.; Lee, G.H.; Yoon, C.; Jeong, U., Kim, Y., Cho, M.H., Kim, D.W. Biodistribution and toxicity of spherical aluminum oxide nanoparticles. J Appl Toxicol. 2016, 36(3), 424-33. doi: 10.1002/jat.3233
51. Katsnelson, B.A.; Privalova, L.I.; Gurvich, V.B.; Kuzmin, S.V.; Kireyeva, E.P.; Minigalieva, I.A.; Sutunkova, M.P.; Loginova, N.V.; Yarushin, S.V.; Soloboyeva, J.I.; Kochneva, N.I. Enhancing population's resistance to toxic exposures as an auxilliary tool of decreasing environmental and occupational health risks (a self-overview). J Environmental Protection. **2014**, 5, 1435–1449. doi:10.4236/jep.2014.514137
52. Privalova, L.I.; Katsnelson, B.A.; Sutunkova, M.P.; Minigalieva, I.A.; Gurvich, V.B.; Makeyev, O.H.; Shur, V.Ya.; Valamina, I.E.; Klinova, S.V.; Shishkina, E.V.; Zubarev, I.V. Looking for biological protectors against adverse health effects of some nanoparticles that can pollute workplace and ambient air (a summary of authors' experimental results). J Environmental Protection. **2017**, 8, 844-866. doi.org/10.4236/jep.2017.88053.
53. Varaksin, A.N.; Katsnelson, B.A.; Panov, V.G.; Privalova, L.I.; Kireyeva, E.P.; Valamina, I.E.; Beresneva O.Y. Some considerations concerning the theory of combined toxicity: a case study of subchronic experimental intoxication with cadmium and lead. Food and Chem. Toxicol. **2014**, 64, 144–156.
54. Katsnelson, B.A.; Minigaliyeva, I.A.; Panov, V.G.; Privalova, L.I.; Varaksin, A.N.; Gurvich, V.B.; Sutunkova, M.P.; Shur, V.Ya.; Shishkina, E.V.; Valamina, I.E.; Makeyev, O.H. Some patterns of metallic nanoparticles' combined subchronic toxicity as exemplified by a combination of nickel and manganese oxide nanoparticles. Food and Chem. Toxicol. 2015, 86, 351-364.
55. Panov, V.G.; Katsnelson, B.A.; Varaksin, A.N.; Privalova, L.I.; Kireyeva. E.P.; Sutunkova, M.P.; Valamina, I.E.; Beresneva, O.Yu. Further development of mathematical description for combined toxicity: A case study of lead–fluoride combination. Toxicol. Rep. 2015, 2, 297–307.
56. Minigalieva, I.A; Katsnelson, B.A.; Panov, V.G.; Varaksin, A.N.; Gurvich, V.B., Privalova, L.I.; Sutunkova, M.P.; Klinova, S.V. Experimental study and mathematical modeling of toxic metals combined action as a

Preprints (www.preprints.org) | NOT PEER-REVIEWED | Posted: 25 January 2018 doi:10.20944/preprints201801.0238.v1

Peer-reviewed version available at Int. J. Mol. Sci. 2018, 19, 837; doi:10.3390/ijms19030837

970 scientific foundation for occupational and environmental health risk assessment. A summary of results
971 obtained by the Ekaterinburg research team (Russia). Toxicol Rep. **2017**, 4C, 194-201.
972 57. Myers, R.H.; Montgomery, D.C.; Anderson-Cook, Ch.M. Response Surface Methodology. John Wiley &
973 Sons, Inc. **2009**
974 58. Panov, V.G.; Varaksin, A.N.; Minigalieva, I.A.; Katsnelson, B.A. The Response Surface Methodology as an
975 approach of choice to modeling and analyzing combined toxicity: theoretical premises, the most important
976 inferences, experimental justification. Biom Biostat J. **2017**, 1(1), 112.-124.
977 59. Katsnelson, B.A.; Panov, V.G.; Minigaliyeva, I.A.; Varaksin, A.N.; Privalova, L.I.; Slyshkina, T.V.;
978 Grebenkina, S.V. Further development of the theory and mathematical description of combined toxicity:
979 an approach to classifying types of action of three-factorial combinations (a case study of manganese-
980 chromium-nickel subchronic intoxication). Toxicology. **2015**, 334, 33-44.
981 60. Canbay, A.; Feldstein, A.; Higuchi, H.; Werneburg, N.; Grambihler, A.; Bronk, S.F.; Gores, G.J. Kupffer
982 cell engulfment of apoptotic bodies stimulates death ligand and cytokine expression. Hepatology. **2003**, 38,
983 1188–1198.